LIMNOLOGY and OCEANOGRAPHY

ASLO

Limnol. Oceanogr. 64, 2019, 1651–1671

doi: 10.1002/lno.11142

Survival under conditions of variable food availability: Resource utilization and storage in the cold-water coral *Lophelia pertusa*

Sandra R. Maier,[1*] **Tina Kutti**,[2] **Raymond John Bannister**,[2] **Peter van Breugel**,[1] **Pieter van Rijswijk**,[1] **Dick van Oevelen**[1]

[1]Department of Estuarine and Delta Systems, Royal Netherlands Institute for Sea Research (NIOZ-Yerseke), Utrecht University, Yerseke, The Netherlands

[2]Benthic resources and processes, Institute for Marine Research, Bergen, Norway

Abstract

Cold-water coral (CWC) reefs are hotspots of biodiversity and productivity in the deep sea, but their distribution is limited by the availability of food, which undergoes complex local and temporal variability. We studied the resource utilization, metabolism, and tissue storage of CWC *Lophelia pertusa* during an experimentally simulated 3-day food pulse, of $^{13}C^{15}N$-enriched phytodetritus, followed by a 4-week food deprivation. Oxygen consumption (0.145 μmol O_2 [mmol organic carbon {OC}]$^{-1}$ h^{-1}), release of particulate organic matter (0.029 μmol particulate organic carbon [POC] [mmol OC]$^{-1}$ h^{-1} and 0.005 μmol particulate organic nitrogen [mmol OC]$^{-1}$ h^{-1}), ammonium excretion (0.004 μmol NH_4^+ [mmol OC]$^{-1}$ h^{-1}), tissue C and N content, and fatty acid (FA) and amino acid composition did not change significantly during the experiment. Metabolization of the labeled phytodetritus, however, underwent distinct temporal dynamics. Initially, *L. pertusa* preferentially used phytodetritus-derived C for respiration (2.2 ± 0.36 nmol C [mmol OC]$^{-1}$ h^{-1}) and mucus production (0.94 ± 0.52 nmol C [mmol OC]$^{-1}$ h^{-1}), but those tracer fluxes declined exponentially to <20% within 2 weeks after feeding and then remained stable, indicating that the remainder of the incorporated phytodetritus had entered a tissue pool with lower turnover. Analysis of ^{13}C in individual FAs revealed a mismatch between the FAs incorporated from phytodetritus and the FA requirements of the coral. We suggest that feeding on other resources, such as lipid-rich zooplankton, could fill this deficiency. A release of 10% of their total OC as respired C and POC during the 4-week food deprivation underlines the importance of regular food pulses for CWC reefs.

Scleractinian cold-water corals (CWCs) such as *Lophelia pertusa* build three-dimensional reef-frameworks (Freiwald 2002; Freiwald et al. 2004; Roberts et al. 2006), which form one of the most diverse and metabolically active ecosystems of the deep sea (Jonsson et al. 2004; Van Oevelen et al. 2009; White et al. 2012). Their geographical distribution in the deep sea is limited, among others, by food availability (Frederiksen et al. 1992; Mortensen et al. 2001; Thiem et al. 2006; Davies et al. 2008). CWCs rely on organic matter produced in the sunlit surface ocean, including fresh phytodetritus and zooplankton, as shown by their stable isotope and fatty acid (FA) composition (Duineveld et al. 2004, 2007, 2012; Kiriakoulakis et al. 2005; Carlier et al. 2009). Organic matter from the surface of the ocean sinks and undergoes microbial degradation in the water column, so that typically only a small percentage reaches the deep-sea floor (Suess 1980; Karl et al. 1988). Several hydrodynamic processes locally and temporally enhance food delivery to the CWC reefs, including tidally controlled rapid downwelling of surface water (Davies et al. 2009; Duineveld et al. 2012), Ekman transport (Thiem et al. 2006), breaking internal waves (Frederiksen et al. 1992; Mienis et al. 2007), and tidally controlled lateral advection of particle-rich bottom water (Duineveld et al. 2007, 2012; Davies et al. 2009). Stimulated by bottom topographies including the CWC reefs and mounds (Soetaert et al. 2016), those hydrodynamic processes can deliver large amounts of fresh organic material to the CWCs in a short period of time, resulting in pulses of higher food availability.

Depending on the location, food delivery is also subject to seasonal cycles. In temperate areas, a temporal mismatch between the phytoplankton and zooplankton production during the spring bloom can lead to a flux of fresh, ungrazed phytoplankton biomass to the seafloor (Thiem et al. 2006; Duineveld et al. 2007; Davies et al. 2009). Subsequent stratification of the water column in summer, which reduces the

*Correspondence: sandra.maier@nioz.nl

surface-to-bottom connectivity (Findlay et al. 2013; Guihen et al. 2018; Van Engeland et al. 2019), and low primary production in winter (Duineveld et al. 2004, 2007; Lavaleye et al. 2009) diminishes the delivery of fresh organic material from the surface to the CWC reefs. During these periods, diurnally migrating and overwintering zooplankton could play a role as food source for CWCs (Heath and Jónasdóttir 2003; Hebbeln et al. 2014; Jónasdóttir et al. 2015; Van Engeland et al. 2019). Nevertheless, zooplankton also undergoes a seasonal succession following the phytoplankton production, with an overall reduced abundance and biomass in winter (Wiborg 1954; Gaard 1999; González-Gil et al. 2015). The widespread distribution of CWCs suggests that they are well-adapted to complex, location-specific, and temporal variations in food availability. Their high flexibility in food utilization, including zooplankton, phytoplankton (detritus), bacteria, even dissolved organic matter (DOM; Mueller et al. 2014; Van Oevelen et al. 2016), and chemoautotrophy (Middelburg et al. 2015) maximizes resource extraction. Dodds et al. (2009) furthermore suggested that a reduction of their metabolic activity may help CWCs overcome periods of reduced food availability. This so-called torpor has been reported for other deep-sea macrofauna, including foraminifera (Linke 1992) and amphipods (Smith and Baldwin 1982; Christiansen and Diel-Christiansen 1993). Larsson et al. (2013*a*), however, found a comparatively low reduction of *L. pertusa* metabolic rates during a 7-month experimental starvation. This indicates a high tolerance to long-term food deprivation and points to a substantial energy-storage capacity, which is supported by high levels of storage lipids in the tissue of CWCs (Dodds et al. 2009; Larsson et al. 2013*a*). Storage lipids mainly consist of triacylglycerols and wax esters, which are built from neutral-lipid-derived fatty acids (NLFAs). In contrast, phospholipid-derived fatty acids (PLFAs) are used to build the structural phospholipids, the major constituents of the cell membrane (Dalsgaard et al. 2003). CWCs have been assumed to build up lipid reserves during the increased food availability following the spring bloom and utilize those reserves in periods of reduced food delivery (Dodds et al. 2009). *Lophelia pertusa* from Mingulay reef did, however, not display a seasonal trend in total amount of storage lipids (Dodds et al. 2009). CWCs could make use of additional carbon storage in carbohydrates, such as glycogen, like anemones (Fitt and Pardy 1981; Ortega et al. 1988; Zamer and Hoffmann 1993) and zooxanthellate corals (Kopp et al. 2015), but this remains to be verified.

The capability of CWCs to deal with variable, temporally reduced food availability physiologically constrains their distribution in the deep sea today and in the future. Increased sea surface temperatures and stratification could reduce primary and export production (Bopp et al. 2001; Gregg et al. 2003; Soetaert et al. 2016) and reinforce the negative energetic consequences of seawater warming and ocean acidification for the calcifying CWCs (Cohen and Holcomb 2009; McCulloch et al. 2012*a*,*b*; Büscher et al. 2017).

In this study, we address how CWC *L. pertusa* metabolizes and stores resources under variable food availabilities. In a stable isotope pulse chase tracer experiment, we exposed the corals to a 3-day experimental food pulse, consisting of ^{13}carbon- and ^{15}nitrogen-enriched phytodetritus, which we followed throughout 4 weeks of food deprivation. The heavy stable isotopes ^{13}C (tracer C) and ^{15}N (tracer N) were traced in corals' tissue, in specific tissue compounds, and in metabolic and excretion products.

Materials and methods

Coral collection and maintenance

Lophelia pertusa colonies were collected on Nakken reef (Hardanger fjord, Norway) on 11 June 2015 during the RV *Håkon Mosby* cruise 2015611, conducted by the Institute of Marine Research (IMR, Bergen). Collection was carried out by the ROV *Aglantha*, run by IMR during this cruise, at 210 m depth at three different sites on Nakken reef (59°49.811′N, 05°33.316′E; 59°49.806′N, 05°33.343′E; 59°49.814′N, 05°33.366′E; maximum distance between stations: 47 m). Corals were transported in cooling boxes with ambient seawater, pumped from 120 m depth at the collection site to the aquarium and lab facilities of Austevoll field station (of the IMR, Bergen, 1.5 h of sailing time from Nakken reef).

Coral colonies were clipped into 24 experimental fragments of similar size with a wire cutter (25 ± 7 polyps, 10 ± 3 g dry mass [DM]), while taking care that each experimental fragment originated from a different colony. Experimental fragments were randomly assigned to a total of eight experimental batches, consisting of three coral fragments each (Fig. 1). The respective, three fragments served as pseudoreplicates within the batches (*see* statistical analyses below) to address the within-batch individual variability of measured tissue parameters. Six additional nonexperimental coral fragments were equally prepared to obtain "field" (in situ) and "start" baseline values of all mentioned tissue parameters. The "field" fragments were sampled immediately after collection and the "start" fragments immediately before the food pulse was applied (*see* experimental design below).

Each of the eight experimental coral batches (three pseudoreplicate fragments each) was maintained in an individual 6.95-liter maintenance chamber, supplied with a flow-through of 0.35-μm-filtered deep fjord water (pumped from 165 m depth close to Austevoll facilities; Langenuen fjord), to maintain "close to" in situ conditions. Regular measurements of temperature (T), salinity (sal), pH, oxygen saturation (O_2 sat), and flow-through rate in all maintenance chambers showed that conditions remained stable throughout the experimental period (T: 8.06 ± 0.02 [SD]°C, sal: 34.75 ± 0.05, pH: 8.43 ± 0.15, O_2 sat: 92.6% air saturation ± 2.8%, flow: 1.1 to 1.4 L min^{-1}).

To prevent water exchange between coral batches, each maintenance chamber received water through a separate hose terminating at the chamber bottom. Water overflowed from the chambers into a 1080-liter-flow-through tank before leaving

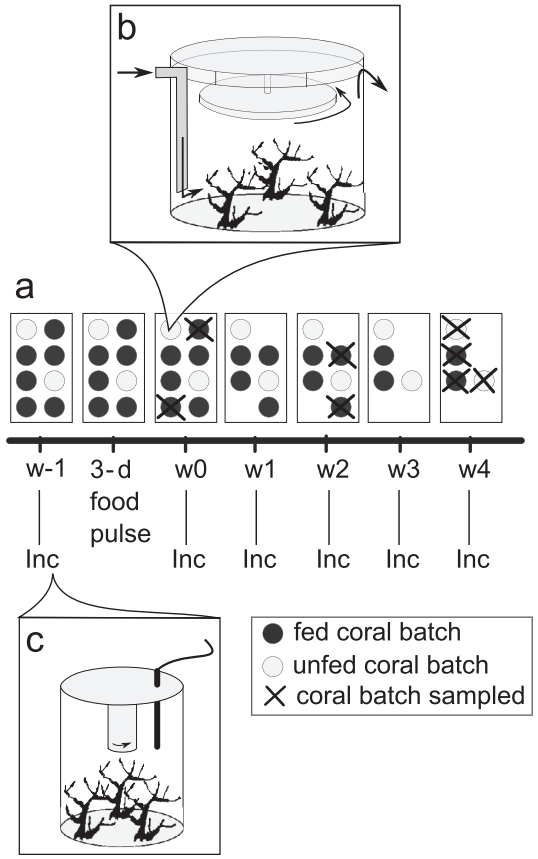

Fig. 1. Experimental design and setup. (**a**) Initially, six fed and two unfed coral batches in their maintenance chambers (filled circles), all partly submersed in a 1080-liter tank (rectangle), over the weeks after feeding ("w-1" to "w4"). Regular incubations (Inc) and sampling (x) of coral batches. (**b**) Maintenance chamber with one coral batch consisting of three pseudoreplicate coral fragments; arrows indicate water movement through chamber via inflow tube and overflow, and circulation of rotating disc. (**c**) Incubation of one coral batch in a closed chamber with stirrer (gray bar) and oxygen sensor (black bar).

the system (Fig. 1). Maintenance chambers were partially (>90%) submerged in this 1080-liter tank to maintain a constant temperature.

Corals were given a recovery time of 13 d from collection to the start of the experiment. During this recovery period, coral batches were regularly fed with fresh zooplankton, collected with a hand-held zooplankton net (350 μm mesh) in Langenuen fjord (38 zooplankton individuals per liter). Feeding was suspended 1 d before the experiment started.

During the experimental period, chambers were regularly cleaned very gently with a syringe to avoid organic matter accumulation within the system. Coral health was monitored through polyp protrusion and tissue sloughing. On average, more than 60% of the polyps per coral batch were protruded.

Preparation of labeled substrate

An axenic culture of the diatom *Skeletonema marinoi* (NIOZ culture collection) was artificially enriched in the stable isotope tracers ^{13}C and ^{15}N to serve as experimental "phytodetritus" food pulse. *Skeletonema marinoi* was grown axenically in twelve 1-liter F/2 culture flasks, containing medium with 0.8 mmol L^{-1} $NaNO_3$ (10 atom% ^{15}N, Cambridge Isotopes) and 2 mmol L^{-1} $NaHCO_3$ (Cambridge Isotopes, 99 atom% ^{13}C), under a 12 h light–12 h dark cycle for 3 weeks to a final cell density of 7.5×10^5 cells mL^{-1} (Mueller et al. 2014). Diatom cells were concentrated on a 0.45 μm cellulose acetate filter (vacuum 200 mbar), flushed into centrifuge tubes with artificial seawater, and centrifuged at 1500 rpm for 10 min. The concentrated diatoms were rinsed three times with artificial seawater to remove residual labeled medium (Mueller et al. 2014). Concentrated labeled diatoms (25.2 atom% ^{13}C, 42.3 atom% ^{15}N, measured as described below for the coral tissue) were kept frozen (–20 °C) until the start of the experiment. Prior to feeding, the diatoms were thawed and thoroughly suspended in 40 mL filtered seawater. This food substrate of dead ^{13}C and ^{15}N-enriched diatoms will be referred to as "(labeled) phytodetritus", and the carbon and nitrogen derived from it as "tracer C" and "tracer N."

Experimental feeding and food deprivation

Six coral batches received a 3-day food pulse of $^{13}C^{15}N$-labeled phytodetritus (week 0, "w0"; Fig. 1) and were subsequently deprived from food for 4 weeks. Two coral batches served as unfed controls. Prior to feeding, the water overflow of the maintenance chambers was stopped, and the water level reduced to 5.9 liter. The phytodetritus food suspension was added with a syringe (1 mmol C [coral batch]$^{-1}$ = 0.17 mmol C L^{-1}, 0.15 mmol N [coral batch]$^{-1}$ = 0.03 mmol N L^{-1}). A rotating disc (diameter 15 cm; Fig. 1) created a current speed in the chamber of approximately 10 cm s^{-1}. Parts of the food particles rapidly accumulated on the chamber floor and were regularly resuspended with a syringe. Corals were allowed to feed for 12 h, after which the water overflow was reintroduced. Remaining food particles were carefully removed from the chambers by syringe to stop the feeding period and avoid accumulation of waste products. This feeding cycle was repeated on three consecutive days, providing the corals with a total of 3 mmol C (coral batch)$^{-1}$.

After the feeding period, corals were maintained in 0.35 μm-filtered seawater (Harmsco filter patron) without being offered additional food for 4 weeks. The 0.35-μm-filter excludes all but picoplankton, e.g., bacterioplankton (Sieburth et al. 1978), and DOM, simulating conditions of reduced particulate food availability.

Weekly closed-cell incubations

At fixed time points, the coral batches (each consisting of three pseudoreplicate coral fragments) were individually incubated in closed chambers: 3 d before feeding (week-1, "w-1"), 12 h after feeding (week 0, "w0"), and 1–4 weeks after feeding ("w1", "w2", "w3", and "w4"; Fig. 1). During each incubation, we measured the "bulk" net fluxes oxygen consumption, ammonium excretion, particulate organic carbon (POC), particulate

organic nitrogen (PON), dissolved organic carbon (DOC), and dissolved organic nitrogen (DON) release. In addition, the metabolic processing of the labeled phytodetritus food pulse was traced by measuring the ^{13}C-respiration (release of ^{13}C-dissolved inorganic C [DIC]) and the release of ^{13}C and ^{15}N-POC and PON (tracer fluxes). As coral batches were sampled at regular intervals, as described in the following paragraph, the number of incubated coral batches decreased over time (Fig. 1). The weekly closed-cell incubations were carried out on two subsequent days, with a maximum of four incubated coral batches per day. To maintain the same time from the feeding, the respective coral batches also received the food pulses with a lag of 24 h.

Prior to each incubation, all incubation chambers and experimental corals were placed in a "100-liter start container" filled with 0.35-μm filtered seawater for about 10 min, from where each coral batch could be transferred into a 1.26-liter incubation chamber without air exposure. Per incubation, two additional incubation chambers without corals served as "filtered-seawater control incubations." After closing the incubation chambers airtight and without air bubbles, they were kept in the 1080-liter-flow-through tank to keep the temperature stable. During the incubation, the oxygen concentration was continuously logged (50 logs min^{-1}) with a FireSting O_2 logger (TeX4, Pyro Science), fitted to each chamber lid. An average incubation time of 10 h (coral incubation: 10.3 h $\pm$ 1.1 h; seawater control incubation: 7.6 h $\pm$ 1.4 h, mean $\pm$ SD) was long enough to detect the targeted bulk fluxes and short enough to avoid a drop in oxygen below 80% air saturation, a conservative threshold for CWC respiration measurements (Dodds et al. 2007). A motor-driven magnetic stirrer created a circular flow and prevented the establishment of concentration gradients of dissolved substances during the incubation. After the incubation, corals were returned to their maintenance chambers.

Water samples for concentrations of DIC (DIC and ^{13}C-DIC), DOC, and ammonium (NH_4^+) were taken in triplicate with a glass syringe at the start of the incubation from the 100-liter start container (start samples) and at the end of the incubation from each incubation chamber (end samples). DIC water samples were transferred into 10 mL headspace vials, fixed with 10 μL of a saturated mercury chloride solution, and stored at 4°C until analysis at NIOZ. DOC water samples were filtered through a precombusted glass fiber filter (GF/F; Whatman, GE Healthcare Life Sciences) into 4 mL acid-washed (10% HCl), precombusted (450°C, 5 h) amber vials and stored at 4°C until analysis at NIOZ. NH_4^+ water samples were filtered through 0.45 μm membrane filters (mixed cellulose esters) into 5 mL polyethylene vials and stored frozen until analysis.

The rest of the incubation water ($\pm$ 250 mL) was filtered through precombusted, preweighed 0.7 μm-GF/F filters (Whatman, n = 3 per incubation chamber) to collect the suspended particulate organic matter (POM) on the filter and determine the concentration and isotope composition of the POC and PON (POC + ^{13}C-POC and PON + ^{15}N-PON; Rix et al. 2016). Filters were frozen, dried to constant weight (40°C) and stored dry and dark until the analysis.

Coral sampling

Two fed coral batches were sampled at each of the following time points: (a) directly after the feeding and the subsequent "w0" incubation, (b) 2 weeks after feeding and the "w2" incubation, and (c) 4 weeks after feeding and the "w4" incubation (Fig. 1). The coral samples were frozen at −20°C, freeze dried, and stored at −20°C until the tissue analysis, including tissue C and N content, tissue composition, and tracer incorporation in tissue, tissue pools, and individual compounds. We here define "tissue pools" as the sum of all neutral-lipid derived fatty acids (NLFAs), phospholipid-derived fatty acids (PLFAs), hydrolysable amino acids (HAAs) and neutral carbohydrates (NCHs), while the term "individual compounds" refers to the individual FAs, HAAs, and NCHs within the respective tissue pools. The two unfed experimental coral batches were sampled after the "w4" incubation. Three additional nonexperimental "field" coral fragments were sampled at "w-1" for "field" (in situ) values of all mentioned tissue parameters. Three additional nonexperimental "start" coral fragments were sampled at "w0" as a reference baseline for the isotopic enrichment to calculate tracer incorporation of fed corals (see below).

Chemical analyses

Coral tissue analysis

Each freeze-dried coral fragment was weighed and homogenized to fine coral powder with a ball mill at a frequency of 30 s^{-1} (MM301, Retsch). To obtain the organic carbon (OC) fraction in the coral tissue, 20–25 mg of the homogenized coral powder (n = 5 per fragment) was transferred to a silver measuring cup, exposed to hydrochloric acid fume (HCl, 37%) under vacuum for 3 d and acidified with drops of increasingly concentrated HCl (2%, 5%, and 30%) until the solution stopped bubbling, indicating successful removal of all inorganic (skeletal) carbon. Samples were dried (50°C), and OC content (in % of DM) and isotope composition (δ^{13}C, in ‰) were analyzed on an elemental analyzer (Flash 1112, THERMO Electron S.p.A.) coupled to an isotope ratio mass spectrometer (EA-IRMS, DELTA-V, THERMO Electron Corporation). There was a high variability within replicate measurements (n = 5 per fragment), so outliers were identified via a Tukey outlier test (with software Excel, 2018) and removed from the dataset. The remaining multiple measurements were averaged per fragment.

Organic nitrogen (ON) content (in % of DM) and nitrogen isotope composition (δ^{15}N, in ‰) were obtained separately from nonacidified 20 mg subsamples of coral powder (n = 3), measured on the EA-IRMS. Due to the lower variability within replicate measurements, no outlier test was performed here.

Analysis of tissue compounds

Total lipids were extracted from ~ 2 g freeze-dried coral powder, and 1 mg freeze-dried phytodetritus, with a modified Bligh-Dyer extraction (Boschker et al. 1999). The chloroform extract was weighed and fractionated on polarity over a silicic acid (Merck) column, by subsequently eluting with 7 mL chloroform, 7 mL acetone, and 15 mL methanol. The chloroform elute contained the NLFAs, and the combined acetone and methanol elutes the PLFAs. Samples for NLFAs and PLFAs were derivatized by mild alkaline methanolysis to fatty acid methyl esters (FAMEs). Individual PLFA-/NLFA-FAMEs were separated with a gas chromatograph (GC, HP G1530) on a BPX70 column (SGE Analytical Science), and their respective concentrations and $\delta^{13}C$ measured on a Finnigan Delta Plus IRMS (THERMO), coupled to the GC via a combustion GC-c-III interface (THERMO; Boschker et al. 1999).

Identification of FAME chromatogram peaks as certain FAs was based on their retention times in relation to the added internal standards C12:0 and C19:0, and omnipresent C16:0, as described in Boschker et al. (1999). In several cases, the identification of the chromatogram peaks as certain FAs was not unique because (a) several FAs coelute (e.g., C13-3-CH_3/C14:0), (b) in two different coral samples, a chromatogram peak of a distinct retention time was allocated to two different FAs—in this case, both FAs were denoted for this peak in both coral samples (e.g., C21:5ω3/C22:3), or (c) in a single coral sample, two subsequent chromatogram peaks with close retention times were allocated to the two same FAs (e.g., C24:1ω9c/C22:5ω3_1 and _2).

HAAs were extracted from 24 to 35 mg coral powder and 2 to 2.8 mg freeze-dried phytodetritus, following Veuger et al. (2005). The subsamples in glass tubes were exposed to HCl fume (37%) for 3 d and subsequently decalcified with drops of 37% HCl. Subsamples were hydrolyzed over night with HCl (6 mol L^{-1} solution) under a nitrogen gas headspace at 110°C and extracts kept frozen (–21°C). The extracts were derivatized with acidified isopropanol and pentafluoropropionic anhydride just prior to the analysis. HAAs were separated on a ZB-5 MS column (Phenomenex), and the HAA-C-concentration and $\delta^{13}C$ signature were measured on the coupled IRMS (Veuger et al. 2005). HAAs were identified based on their retention time in relation to the added internal standard norleucine, according to Veuger et al. (2005). The individual HAA-C-concentrations and $\delta^{13}C$ values were corrected for the C added during derivatization. Most of the 20 "common" L-AAs can be detected with the present method, except for histidine, cysteine, tryptophan, and arginine, because these require a special derivatization method (Erbe 1999). As certain HAAs may be more susceptible to evaporation during the preparation and analysis, a standard HAAs mix (Sigma Aldrich AAS18) was analyzed in the same way as the samples, to determine the percentage recovery for each individual HAA. The HAA-C concentrations measured in the samples were corrected for this recovery. The recovery was >73% for all HAAs besides methionine (30%), which was therefore excluded from the analysis. During the hydrolysis, asparagine is converted to aspartic acid and glutamine to glutamic acid (Uhle et al. 1997; Erbe 1999), so the sum of asparagine and aspartic acid and glutamine and glutamic acid is presented.

NCHs were extracted from 500 mg coral powder following Grosse et al. (2015). Subsamples were mixed with 0.5-mL ultrapure water and decalcified over night by addition of 0.5-mL 11 mol L^{-1} sulfuric acid (H_2SO_4). The solution was diluted with ultrapure water to 1.1 mol L^{-1} H_2SO_4, and carbohydrates were hydrolyzed at 120°C for 1 h. The solution was neutralized with strontium carbonate ($SrCO_3$), and the resulting strontium percarbonate ($SrSO_4$) was removed via centrifugation. Extracts were eluted over a double-bed resin, containing 2 mL of a cation exchange resin and 2 mL of an anion exchange resin (Dowex 50WX8-100, Dowex 1X8Chloride), to remove inorganic and organic salts, filtered over a 0.22 μm filter and stored at –20°C. Carbohydrate components were separated and analyzed for concentration and $\delta^{13}C$ signature via high-performance liquid chromatography (Surveyor, Thermo), using an Aminex HPX-87H Ion Exclusion Column (Biorad), coupled to a Delta-V IRMS via an LC-Isolink interface (Thermo; Grosse et al. 2015). In this configuration, galactose/xylose/fructose/mannose and fucose/ribose/arabinose, respectively, elute together.

Dissolved inorganic carbon

A 3-mL helium gas headspace was created in each headspace vial by injecting helium gas through the septum and simultaneously removing excess sample through another syringe (Moodley et al. 2000). Around 2.5 mL of this excess water was used to determine the DIC concentration on an Apollo SciTech AS-C3. Through addition of 100 μL (10 μL mL^{-1}) concentrated phosphoric acid (H_3PO_4) to the sample in the headspace vial, DIC was completely transformed to gaseous carbon dioxide (CO_2). A glass syringe was used to sample 10 μL of headspace gas, which was subsequently injected in the EA-IRMS as described above, to measure the $\delta^{13}C$ of the CO_2.

Ammonium excretion

Concentration of ammonium (NH_4^+) was measured by applying Berthelot's reaction between ammonium and phenol (Searle 1984) on a SEAL QuAAtro segmented continuous flow analyzer.

Suspended POC, PON, DOC, and DON

GF/F with POC and PON samples were weighed and analyzed on the EA-IRMS for POC and PON concentration in the known volume of filtered water, $\delta^{13}C$ of POC, and $\delta^{15}N$ of PON. DOC concentration in the respective water samples was measured on a Formacs^{HT} Low Temperature Total Organic Carbon Analyser (Skalar).

Calculations

Bulk fluxes

The net bulk fluxes include oxygen (O_2) consumption, ammonium excretion, and release of POC, PON, and DOC. O_2 consumption was calculated from a linear regression of the O_2 concentrations recorded over time during the closed-cell incubation. The resulting slope was multiplied with a respiratory quotient of 1 (Glud et al. 2008) to convert the O_2 consumption rate into (bulk) C respiration. Rates of ammonium excretion and release of POC, PON, and DOC were calculated from the respective concentration change during the closed-cell incubations (concentration in end water sample minus concentration in start water sample). All concentration changes of coral incubations were corrected for the concentration changes measured in the parallel "filtered-seawater-control incubations" and multiplied with the volume of the incubation chamber. Fluxes are expressed per OC content of the respective coral batch (i.e., the sum of the three pseudoreplicate fragments in an incubation).

Tissue composition

The tissue carbon and nitrogen content of the *L. pertusa* fragments was standardized to their DM (i.e., skeleton and tissue), expressed as mmol C or N (g DM)$^{-1}$. Concentrations of each individual HAA, NLFA, PLFA, and NCH are expressed in moles C derived from the respective compound per moles OC of the coral fragment. Only FAs with a concentration >5% of the total NLFA/PLFA concentration in at least one coral fragment are presented separately, while the other FAs were summed as "rest". The individual HAAs, NLFAs, PLFAs, and NCHs were also summed to the tissue pools "total HAAs", "NLFAs", "PLFAs", and "NCHs" of the respective coral fragment.

Tracer incorporation

For tracer C incorporation into coral tissue, the ^{13}C : ^{12}C ratio of the respective coral fragment (R_{sample}) was calculated from measured $\delta^{13}C$ (‰) in the sample via $R_{sample} = ([\delta^{13}C_{sample}/1000] + 1) \times R_{ref}$, with $R_{ref} = 0.0111802$. Fractional abundance of ^{13}C ($F^{13} = {}^{13}C/[{}^{12}C + {}^{13}C]$) was calculated as $F^{13} = R_{sample}/(R_{sample} + 1)$ for experimental coral fragments ($F^{13}{}_{coral}$) and for the three coral fragments sampled at the start of the experiment ($F^{13}{}_{start}$). The enrichment of each experimental coral fragment ($F^{13}E$) was expressed in relation to the average F^{13} of the three start coral fragments as $F^{13}E = F^{13}coral - \overline{F}^{13}start$. The ^{13}C incorporation into each fragment (μmol ^{13}C fragment^{-1}) was obtained by multiplying its $F^{13}E$ with its OC content (moles OC). The total amount of carbon incorporated from the labeled phytodetritus into each fragment (tracer C incorporation, μmol C_{tracer} fragment^{-1}) was calculated by dividing each fragments' ^{13}C incorporation by the fractional abundance F^{13} of the labeled food ($F^{13}{}_{food} = 0.2522818$). The calculation procedure is identical for organic N, for which nitrogen gas served as reference material ($R_{ref} = R_{N2} = 0.0036782$) and $F^{15}{}_{food}$ was 0.4227415. Tracer C and N incorporation rates were normalized to the moles OC of the respective coral fragment and averaged over the three pseudoreplicate fragments per coral batch.

Tracer C incorporation in individual HAAs, NLFAs, PLFAs, and NCHs was calculated correspondingly, from the individual compounds' C-concentration multiplied by its ^{13}C-enrichment relative to the same compound in the unlabeled start coral fragments and divided by $F^{13}{}_{food}$. Two PLFAs (peaks identified as C20:4ω3/C20:5ω3/ecl21.917, C24:1ω9c/C22:5ω3) occurred in several fed coral fragments at a concentration of >5% of their total NLFAs/PLFAs, but were absent from all three start coral fragments. To calculate those compounds' ^{13}C-enrichment, their corresponding $F^{13}{}_{start}$ was estimated as the average of the $F^{13}{}_{start}$ of all other PLFAs >5% of the start coral fragments ($F^{13}{}_{start} = 0.0108 \pm 0.0044$).

Tracer fluxes

Tracer fluxes are the coral-mediated fluxes of C and (if applicable) N originating from the isotopically enriched food pulse during the closed-cell incubations and include tracer C respiration and tracer POC and PON release. All tracer fluxes were calculated from the average bulk concentration of the respective substance in the incubation start and end samples ($\overline{c}$), because the bulk concentrations did not change significantly between start and end sampling (*t*-test, $p > 0.05$). The average concentration of the respective substance (DIC, POC, and PON) was multiplied by its enrichment in the heavy isotope ^{13}C or ^{15}N in the end sample relative to the start sample ($F^{13}E = F^{13}{}_{end\ sample} - F^{13}{}_{start\ sample}$, $F^{15}E = F^{15}{}_{end\ sample} - F^{15}{}_{start\ sample}$) and divided by the food enrichment (see above) to obtain the tracer flux ($\text{Tracer C flux} = \frac{\overline{c} \times F^{13}E}{F^{13}food}$, $\text{Tracer N flux} = \frac{\overline{c} \times F^{15}E}{F^{15}food}$; Moodley et al. 2000). All tracer C and N fluxes were corrected for the tracer C and N fluxes in the respective parallel "filtered-seawater control incubations" and normalized to the moles OC of the respective coral batch.

Statistical analyses

Data were analyzed with linear mixed effect (LME) models in RStudio, Version 0.98.1103 (2009–2014 RStudio; R Core Team, 2017), using the nonlinear mixed effect (NLME) models (Pinheiro et al. 2017). LME can cope with the unbalanced design (Crawley 2007; Pinheiro et al. 2017), which is relevant for this study because in w0, w2, and w4, respectively, two coral batches were sacrificed, reducing the amount of replicate coral batches for bulk and tracer fluxes (Fig. 1). Furthermore, it allows nesting of the three coral pseudoreplicate "fragments" in the respective coral "batch."

The dependent variables (1) bulk fluxes, (2) tracer fluxes, (3) tissue C and N content, (4) tissue composition (C concentration in tissue pools NLFAs, PLFAs, HAAs, and NCHs and individual compounds within tissue pools), and (5) tracer incorporation in tissue and compounds (tissue pools and individual compounds within tissue pools) were analyzed for the fixed factors (a) "feed," i.e., difference between fed and unfed corals, and (b) "week",

i.e., changes with time (after the food pulse). In case of the C concentration and tracer C incorporation in the individual compounds within a tissue pool, the respective compounds (e.g., all FAs derived from neutral lipids) constituted multiple dependent variables. "Bulk and tracer fluxes" encompass the respective measurements on the experimental coral batches from week-1 (w-1) to week 4 (w4), while all tissue parameters refer to the respective measurements on coral fragments nested in coral batches at w-1, w0, w2, and w4. In the latter, measurements on the "field" coral batch were included in the statistical analysis, while measurements on the "start" coral batch were left out as they were already used to calculate the tracer C incorporation of the fed coral batches. Random effects in the analysis of bulk and tracer fluxes are "batch," i.e., the respective coral batch, nested in "week" to control for repeated measurements of fluxes on the same coral batches over time (weeks). Random effects in the analysis of tissue parameters are "fragment" nested in coral "batch" (with three coral fragments per batch; Fig. 1). Data were checked for heteroscedasticity with the Fligner–Killeen test (Crawley 2007). If the assumption of homoscedasticity was not fulfilled, data were still tested for significance, but the heteroscedasticity was denoted and the results carefully interpreted. Nonsignificant effects were subsequently excluded from the LME up to the minimum adequate model (Crawley 2007). Probabilities and *t* distributions were noted from the last updated model where at least one of the fixed factors ("feed" or "week") still occurred, which was not necessarily the minimum adequate model, if neither of the fixed factors showed a significant effect. Effects were considered significant on a significance level of $\alpha = 95\%$ (probability $p < 0.05$).

Additionally, bulk and tracer fluxes were integrated over the 4 weeks of food deprivation, following the food pulse to estimate corals' integrated total bulk C and N release and their total release of the food tracer C and N. Therefore, additional models were fitted for fed and unfed corals separately and integrated. These models include LME models for the bulk fluxes from w0 to w4 and exponential decay functions implemented with NLME for the tracer fluxes of fed corals from w0 to w4. Fixed effects are "week" for the LMEs and the estimated model parameters *a* and *b* for the NLMEs, whereas the random effects for both model types are "batch" nested in "week."

All values are given in average ± standard deviation.

Results

Bulk fluxes

Oxygen consumption and ammonium excretion rates of neither fed nor unfed coral batches changed with time (Fig. 2a,b; Table 1). Fed coral batches showed significantly higher 4-week average oxygen consumption and ammonium release rates (0.146 ± 0.026 μmol O_2 [mmol OC]$^{-1}$ h^{-1} and 0.004 ± 0.001 μmol NH_4^+ [mmol OC]$^{-1}$ h^{-1}) as compared to the unfed coral batches (0.111 ± 0.042 μmol O_2 [mmol OC]$^{-1}$ h^{-1} and 0.003 ± 0.001 μmol NH_4^+ [mmol OC]$^{-1}$ h^{-1}).

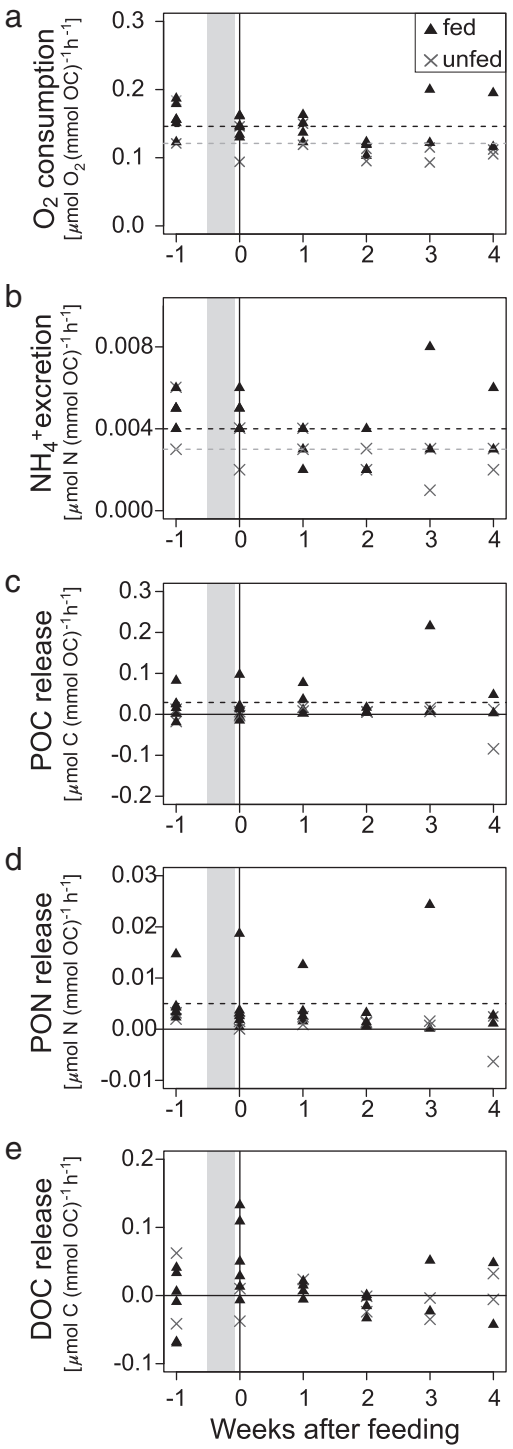

Fig. 2. Hourly bulk oxygen, carbon, and nitrogen fluxes per mmol OC of fed (black triangles) and unfed (gray "x") coral batches, over the "weeks" after the phytodetritus food pulse (gray bar). (a) Oxygen consumption, (b) ammonium excretion, and release of (c) particulate organic carbon, (d) particulate organic nitrogen and (e) dissolved organic carbon. Dashed lines: minimum adequate models.

Table 1. Results of the LME models testing the dependent variables (Par) for the fixed effects "week" (weeks after feeding) and "feed" (fed vs. unfed coral batches).

			LME fed vs. unfed vs. week					
Group	**Par**	**Unit**	**Fixed effect**	**Value**	**SE**	**df**	***t***	***p***
Bulk fluxes	Resp	μmol O_2 (mmol OC)$^{-1}$ h^{-1}	Week	0.00	0.00	4	−1.32	0.26
			Feed	−0.02	0.01	29	−2.79	***0.01***
	POC	μmol C (mmol OC)$^{-1}$ h^{-1}	Week	0.00	0.01	4	0.44	0.68
			Feed	−0.03	0.02	29	−2.01	0.05
	DOC*	μmol C (mmol OC)$^{-1}$ h^{-1}	Week	0.00	0.01	4	−0.31	0.78
			Feed	−0.01	0.01	29	−0.85	0.40
	NH_4	μmol N (mmol OC)$^{-1}$ h^{-1}	Week	0.00	0.00	4	−1.28	0.27
			Feed	0.00	0.00	29	2.35	***0.03***
	PON	μmol N (mmol OC)$^{-1}$ h^{-1}	Week	0.00	0.00	4	−0.60	0.58
			Feed	0.00	0.00	29	−2.15	***0.04***
Tracer fluxes	Resp*	nmol C (mmol OC)$^{-1}$ h^{-1}	Week	−0.02	0.16	4	−0.13	0.90
			Feed	−0.91	0.15	29	−6.13	***0.00***
	POC*	nmol C (mmol OC)$^{-1}$ h^{-1}	Week	−0.04	0.07	4	−0.53	0.63
			Feed	−0.27	0.10	29	−2.66	***0.01***
	PON*	nmol N (mmol OC)$^{-1}$ h^{-1}	Week	0.00	0.01	4	−0.42	0.69
			Feed	−0.04	0.01	29	−2.95	***0.01***
Tissue C and N content	C	mmol C (g DM)$^{-1}$	Week	−0.01	0.05	6	−0.17	0.87
			Feed	−0.20	0.17	7	−1.18	0.28
	N	mmol N (g DM)$^{-1}$	Week	0.00	0.00	6	0.23	0.83
			Feed	−0.02	0.02	7	−1.13	0.29

df, degrees of freedom; *p*, probability (bold italic: significant on a significance level of α = 95%); SE, Standard error; *t*, T distribution; Value, estimate effect value (in the indicated unit).
*Homoscedasticity.

POC and PON release of both fed and unfed coral batches did not change over the 4 weeks of food deprivation (Fig. 2c,d; Table 1). Fed coral batches showed higher 4-week average POC and PON release rates (0.029 ± 0.049 μmol POC [mmol OC]$^{-1}$ h^{-1} and 0.005 ± 0.006 μmol PON [mmol OC]$^{-1}$ h^{-1}) than unfed coral batches (−0.002 ± 0.028 μmol POC [mmol OC]$^{-1}$ h^{-1} and 0.001 ± 0.002 μmol PON [mmol OC]$^{-1}$ h^{-1}), which was significant only for PON release (Table 1). DOC release of both fed and unfed coral batches was variable and ranged around zero (Fig. 2e; fed: 0.012 ± 0.047 and unfed: −0.001 ± 0.031 μmol DOC [mmol OC]$^{-1}$ h^{-1}).

Four weeks after feeding on the phytodetritus food pulse, fed *L. pertusa* had an integrated 4-week bulk C release of 0.118 mmol C (mmol OC)$^{-1}$ (4 weeks)$^{-1}$ or 0.126 mmol C (g DM)$^{-1}$ (4 weeks)$^{-1}$ and a N release of 0.006 mmol N (mmol OC)$^{-1}$ (4 weeks)$^{-1}$ or 0.007 mmol N (g DM)$^{-1}$ (4 weeks)$^{-1}$ (Fig. 3a), calculated from the minimum adequate models as shown in Table 3. More than 80% of the bulk C release was by respiration, the remainder by POC release, while DOC release was not significant (Table 1).

Bulk tissue composition

The OC and ON content of the two *L. pertusa* batches sampled after 4 weeks of food deprivation was ~ 20% lower (0.92 ± 0.27 mmol OC [g DM]$^{-1}$ and 0.13 ± 0.03 mmol ON [g DM]$^{-1}$) than in the two batches sampled directly after feeding (1.19 ± 0.40 mmol OC [g DM]$^{-1}$ and 0.14 ± 0.05 mmol ON [g DM]$^{-1}$; Fig. 3), but that difference was not significant due to the high variability in the data (Table 1). One fragment of a fed coral batch showed signs of tissue sloughing in the fourth week of food deprivation.

About 40% of the total OC in the tissue of *L. pertusa* could be accounted for by the compound-specific analysis (sum of all C in measured tissue compounds). Directly after feeding (week 0), *L. pertusa* contained 11% of its OC as HAAs, 23% as NLFAs, 4% as PLFAs, and 1% as NCHs (Fig. 3a). Phytodetritus carbon was composed of 31% HAAs, 2% NLFAs, and 6% PLFAs (NCHs were not measured here). Both in the NLFA and the PLFA pool, corals contained most OC as highly unsaturated fatty acids (HUFAs, with an equal or more than four double bonds), while phytodetritus contained most organic NLFA- and PLFA-C as polyunsaturated fatty acids (PUFAs; two to three double bonds; Table 4). The NLFA pool of the corals comprised relatively more monounsaturated fatty acids (MUFAs) than the PLFA pool (Table 4).

After 4 weeks of food deprivation, corals contained on average 13% less C in the NLFA pool and 36% more in the HAA pool (Fig. 3a), but this trend was not significant, and the amount of C in all biochemical tissue pools HAAs, NLFAs, PLFAs, and NCHs did not change significantly over time,

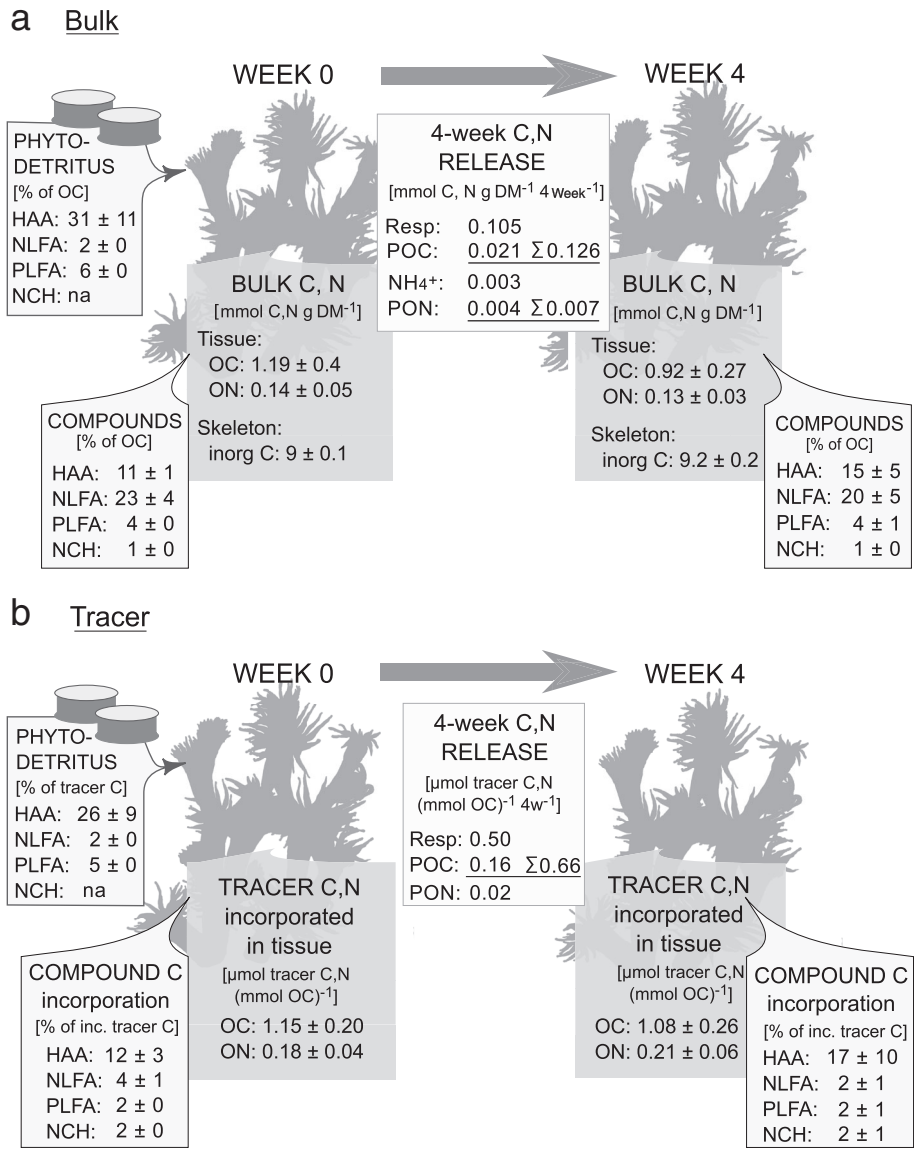

Fig. 3. Bulk (**a**) and tracer (**b**) C and N budget of *L. pertusa* directly after feeding on phytodetritus (week 0) and after 4 weeks of subsequent food deprivation (week 4). Bulk/tracer C, N in coral tissue, tissue composition (compounds), composition of "phytodetritus" food, and corals' 4-week C, N release as respired C (Resp), and released "POC" and "PON". One gram coral DM ≈ 0.92–1.19 mmol OC.

neither did the individual compounds within these tissue pools (Table 2; Fig. 4a,c,e,g).

Tracer fluxes

Fed *L. pertusa* respired carbon from the phytodetritus food pulse, shown clearly by their enhanced tracer C respiration after feeding (week 0) compared to before feeding (week 1; Fig. 5a) and by the significant difference in respired tracer C between fed and unfed corals at week 0 (Table 1; Fig. 5a). Tracer C respired by fed corals was highest 12 to 24 h after feeding (week 0, 2.2 ± 0.36 nmol tracer C [mmol OC]$^{-1}$ h^{-1}) and declined exponentially with time (Table 3) to 0.47 ± 0.1 nmol tracer C (mmol OC)$^{-1}$ h^{-1} 4 weeks after feeding.

Tracer carbon and nitrogen was detected in the POM released by fed corals (Fig. 5b,c). The release of POC and PON originating from the phytodetritus food (i.e., tracer POC and PON) showed the same trend as respired tracer carbon, with highest values 12 to 24 h after feeding (0.94 ± 0.52 nmol tracer POC released [mmol OC]$^{-1}$ h^{-1} and 0.12 ± 0.06 nmol tracer PON released [mmol OC]$^{-1}$ h^{-1}) and an exponential decline (Table 3) to almost zero 4 weeks after feeding (0.08 ± 0.02 nmol tracer POC released [mmol OC]$^{-1}$ h^{-1} and 0.02 ± 0.001 nmol tracer PON released [mmol OC]$^{-1}$ h^{-1}).

The integrated C budget, based on the minimum adequate models over 4 weeks after feeding on the phytodetritus food pulse (Table 3), revealed that *L. pertusa* respired 43% of the incorporated isotopically enriched C, released 14% as POC

Table 2. Results of the LME model, part 2.

			LME fed vs. unfed vs. week					
Group	**Par**	**Unit**	**Fixed**	**Value**	**SE**	**df**	***t***	***p***
Tissue composition: C in tissue pools (sum of resp. compounds)	Σ HAAs	μmol C (mmol OC)$^{-1}$	Week	2.45	4.04	2	0.61	0.61
			Feed	6.63	15.61	4	0.42	0.69
	Σ NLFAs	μmol C (mmol OC)$^{-1}$	Week	−9.86	7.89	2	−1.25	0.34
			Feed	−11.98	25.53	4	−0.51	0.64
	Σ PLFAs	μmol C (mmol OC)$^{-1}$	Week	1.24	1.90	2	0.66	0.58
			Feed	−8.93	7.34	4	−1.22	0.29
	Σ NCHs	μmol C (mmol OC)$^{-1}$	Week	0.43	0.23	2	1.84	0.21
			Feed	−0.56	1.09	4	−0.51	0.64
Tissue composition: C in individual compounds (within tissue pools)	HAAs*	μmol C (mmol OC)$^{-1}$	Week	0.25	0.25	2	0.99	0.43
			Feed	0.09	1.00	4	0.09	0.93
	NLFAs*	μmol C (mmol OC)$^{-1}$	Week	−2.67	1.51	2	−1.77	0.22
			Feed	−1.38	6.60	4	−0.21	0.84
	PLFAs*	μmol C (mmol OC)$^{-1}$	Week	0.05	0.37	2	0.14	0.90
			Feed	−1.97	1.40	4	−1.40	0.23
	NCHs*	μmol C (mmol OC)$^{-1}$	Week	0.06	0.07	2	0.79	0.51
			Feed	−0.22	0.29	4	−0.76	0.49
Tracer incorp. in tissue	C*	μmol C (mmol OC)$^{-1}$	Week	−0.01	0.02	6	−0.45	0.67
			Feed	−1.10	0.09	7	−12.64	***0.00***
	N*	μmol N (mmol OC)$^{-1}$	Week	0.00	0.01	6	0.70	0.51
			Feed	−0.20	0.02	7	−8.86	***0.00***
Tracer incorp. in tissue pools	Σ HAAs*	nmol C (mmol OC)$^{-1}$	Week	5.01	7.13	2	0.71	0.55
			Feed	−151.52	27.76	4	−5.46	***0.01***
	Σ NLFAs	nmol C (mmol OC)$^{-1}$	Week	−3.88	1.21	2	−3.21	*0.09*
			Feed	−21.59	5.39	4	−4.01	***0.02***
	Σ PLFAs*	nmol C (mmol OC)$^{-1}$	Week	−0.61	1.30	2	−0.47	0.68
			Feed	−24.04	4.54	4	−5.30	***0.01***
	Σ NCHs*	nmol C (mmol OC)$^{-1}$	Week	0.70	1.34	2	0.49	0.67
			Feed	−24.25	4.22	4	−5.75	***0.00***
Tracer incorp. in individual compounds (within tissue pools)	HAAs*	nmol C (mmol OC)$^{-1}$	Week	0.77	0.41	2	1.88	0.20
			Feed	−11.47	1.92	4	−5.98	***0.00***
	NLFAs*	nmol C (mmol OC)$^{-1}$	Week	−1.55	0.57	2	−2.71	0.11
			Feed	−0.56	2.66	4	−0.21	0.84
	PLFAs*	nmol C (mmol OC)$^{-1}$	Week	−0.21	0.18	2	−1.18	0.36
			Feed	−2.94	0.75	4	−3.92	***0.02***
	NCHs	nmol C (mmol OC)$^{-1}$	Week	0.28	0.90	2	0.31	0.78
			Feed	11.98	2.05	4	−5.84	***0.00***

df, degrees of freedom; *p*, probability (bold italic: significant on a significance level of α = 95%); SE, Standard error; *t*, T distribution; Value, estimate effect value (in the indicated unit).
*Homoscedasticity.

(Fig. 3b), and released 11% of the incorporated N as PON (Fig. 3b). The integrated 4-week tracer C release (0.66 μmol tracer C [mmol OC]$^{-1}$ [4 weeks]$^{-1}$; Fig. 3b) constitutes 0.5% of the 4-week bulk C release (Fig. 3a).

Tracer incorporation into tissue

All fed *L. pertusa* fragments incorporated tracer carbon and nitrogen from the 3-day phytodetritus food pulse in their tissue (Fig. 6a,b). Unfed corals did not show tracer C and N incorporation into their tissue, and the tracer C and N incorporation was significantly different between all fed and all unfed coral batches (Fig. 6a,b; Table 2), indicating that the experimental setup successfully prevented cross contamination between the coral maintenance chambers. Directly after feeding at week 0, fed coral batches had incorporated a total of 1.15 ± 0.20 μmol tracer C (mmol OC)$^{-1}$, or 0.38 ± 0.07 μmol tracer C (mmol OC)$^{-1}$ 12 h^{-1}, and a total of 0.18 ± 0.04 μmol tracer N (mmol OC)$^{-1}$, or 0.06 ± 0.01 μmol

Table 3. Statistics of LME and NLME models for integration of bulk and tracer fluxes.

			Fed corals vs. week		Unfed corals vs. week	
Group	Par	Type	Model	Statistics of model parameters	Model	Statistics of model parameters
Bulk fluxes	Resp	LME	Resp=0.145*	*I*: t=20.80, p=0, df=18	Resp=0.118	*I*: t=14.76, p=0, df=6
	POC	LME	POC=0.029*	*I*: t=2.85, p=0.01, df=18	None	na
	DOC	LME	None	na	None	na
	NH4	LME	NH_4=0.004*	*I*: t=8.30, p=0, df=18	NH_4=0.003	*I*: t=8.40, p=0, df=6
	PON	LME	PON=0.005	*I*: t=3.84, p=0.00, df=18	na	na
Tracer fluxes	Resp	NLME	Resp=2.219×exp(−0.665×week)	*a*: t=14.25, p=0; *b*: t=6.82, p=0; df=11	na	na
	POC	NLME	POC=0.842×exp(−0.954×week)*	*a*: t=8.78, p=0; *b*: t=10.47, p=0; df=11	na	na
	PON	NLME	PON=0.122×exp(−1.394×week)*	*a*: t=5.11, p=0; *b*: t=5.95, p=0; df=11	na	na

a, *b*, parameters of exponential model $y = a \times \exp(-b \times x)$; I, intercept; model, fitted minimum adequate model; na, integration not applicable; none, no minimum adequate model significant; resp, respiration.
*The assumption of heteroscedasticity was not fulfilled.

Table 4. Average percentage of bulk and tracer carbon in HUFAs, PUFAs, MUFAs, and SFAs in the NLFAs and PLFAs of fed corals and phytodetritus.

		NLFAs					PLFAs				
Organism	C-pool	Uncat	SFAs	MUFAs	PUFAs	HUFAs	Uncat	SFAs	MUFAs	PUFAs	HUFAs
Fed corals	Bulk C	25	19	21	0	35	35	6	7	0	51
	Tracer C	−21	44	22	0	56	32	9	8	0	50
Phytodetritus	Bulk C	7	23	15	41	15	0	29	12	37	21
	Tracer C	7	19	10	50	14	0	30	8	37	25

Uncat, FAs not clearly assignable (FAs <5% C, coeluting FAs falling in two categories, unidentified FAs).

tracer N (mmol OC)$^{-1}$ 12 h^{-1}. This adds up to 1.4% of the total food C and N that was added during the total feeding period (0.47% [12 h]$^{-1}$) and 0.1% of OC and ON of the coral. The amount of tissue-incorporated tracer C and N did not change significantly with time (Fig. 6a,b). Four weeks after feeding, the tissue of the fed coral batches contained 1.08 ± 0.26 μmol tracer C (mmol OC)$^{-1}$ and 0.21 ± 0.06 μmol tracer N (mmol OC)$^{-1}$.

Tracer incorporation into specific tissue compounds

Biochemical tissue pools

A total of 19% of the phytodetritus C, which *L. pertusa* incorporated in its tissue, could be traced back to the tissue pools (Fig. 3b). Compared to their bulk tissue composition, corals allocated relatively little C to the NLFAs (4% of the total incorporated tracer C) and relatively more to the HAAs (23% of the total incorporated tracer C; Fig. 3). The phytodetritus likewise contained only 2% of the tracer C in NLFAs and 26% in HAAs (Fig. 3b).

The tracer C in neither of the biochemical tissue pools changed significantly over the 4 weeks of food deprivation and neither did the tracer C in the individual compounds within the respective tissue pools (Fig. 4; Table 2).

Hydrolysable amino acids

Tracer C incorporation into individual HAAs from w0 to w4 (Fig. 4b) largely corresponded to the bulk HAA-carbon composition of the coral (Fig. 4a). Most tracer C was incorporated in glutamic acid/glutamine, closely followed by aspartic acid/asparagine and leucine (Fig. 4b). Some individual HAAs were relatively more (e.g., valine and isoleucine) or less (e.g., glycine and proline) abundant in the corals than in the phytodetritus, but those differences amounted to less than 10% per compound (Fig. 7a). Corals preferably incorporated HAAs from phytodetritus (Fig. 7b), which were more abundant in their tissue, such as valine and isoleucine (Fig. 7a). Those HAAs show a higher relative tracer incorporation in corals than in their phytodetritus food (Fig. 7b). Glycine and proline were relatively less abundant in the coral tissue than in the phytodetritus food (Fig. 7a) and likewise show a lower relative tracer incorporation in corals than in their phytodetritus food, which indicates that corals selected

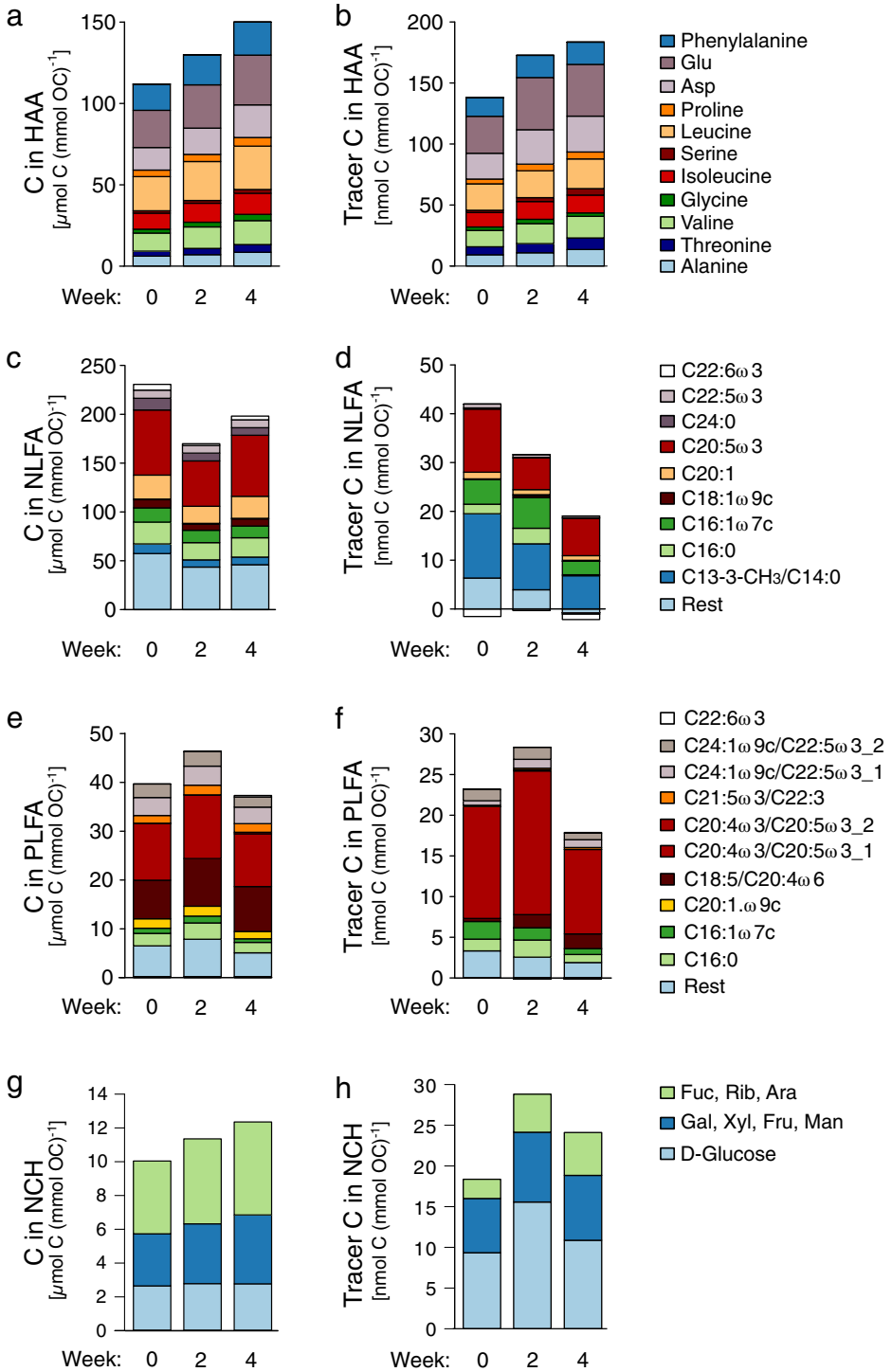

Fig. 4. Individual HAAs, NLFAs, PLFAs, and NCHs per mmol OC of fed coral batches over the weeks after feeding (week). (**a**, **c**, **e**, **g**) Bulk C concentration in HAAs, NLFAs, PLFAs, and NCHs. (**b**, **d**, **f**, **h**) Tracer C incorporated in HAAs, NLFAs, PLFAs, and NCHs. Abbreviations: Ara, arabinose; Asp, asparagine/aspartic acid; Fru, Fructose; Fuc, fucose; Gal, galactose; Glu, glutamine/glutamic acid; Man, Mannose; Rest, FAs <5% C-concentration; Rib, ribose; Xyl, Xylose.

against those HAAs (Fig. 7b). Alanine, threonine, and serine were present in corals bulk tissue at similar proportions compared to their phytodetritus food and incorporated accordingly (Fig. 7a,b). The only marked differences in tracer C allocation compared to their bulk composition occurred in glutamic acid/glutamine and aspartic acid/asparagine, for which tracer C allocation indicated preferential incorporation, and in leucine and phenylalanine, which corals selected against.

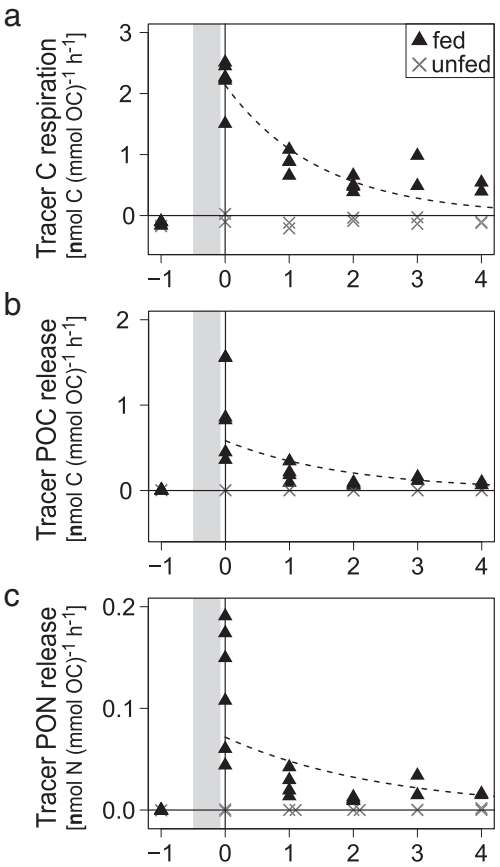

Fig. 5. Hourly tracer carbon and nitrogen fluxes per mmol OC of fed (black triangles) and unfed (gray "x") coral batches, over the weeks after the phytodetritus food pulse (gray bar). (a) tracer C respiration, and release of (b) tracer POC, and (c) tracer PON. Dashed line: minimum adequate model.

Neutral- and phospholipid-derived fatty acids

The phytodetritus food generally contained more short/medium-chain FAs (from C13 to C20), while the coral tissue was very low in those FAs (<5% of the total FA-C; Fig. 7c,e), and the FA incorporation followed this pattern (Fig. 7d,f). *Lophelia pertusa* was characterized by more long-chain FAs (>C20), some of which were only present in the corals and not in their phytodetritus food (Fig. 7c,e). Tracer C incorporation into those longer chain FAs indicates de novo synthesis by the coral (Fig. 7d,f).

Both in the NLFA pool and especially in the PLFA pool, corals incorporated proportionally most tracer C from the phytodetritus food in C20:5ω3 or C20:4ω3/C20:5ω3 (Figs. 4d,f, 7d,f). Shorter chain FAs from C13:3-methyl/C14:0 to C16:1ω7c were more incorporated in the NLFA than in the PLFA pool. In the PLFA pool, C18:5/C20:4ω6 was incorporated at a much lower proportion than present in the bulk PLFA pool, and C20:1ω9c and C21:5ω3/C22:3 were almost not incorporated.

Both for the NLFAs and the PLFAs, HUFAs (with an equal or more than four double bonds) showed the highest share of corals' tracer C incorporation from the phytodetritus food, where PUFAs (two to three double bonds) constituted the dominant FA class (Table 4).

Neutral carbohydrates

Most tracer C in the NCH pool was found in D-glucose, followed by galactose/xylose/fructose/mannose and fucose/ribose/arabinose (Fig. 4h). Tracer C incorporation into D-glucose (Fig. 4h) was relatively higher than the D-glucose found in the bulk tissue (Fig. 4g).

Discussion

We studied the carbon and nitrogen metabolization and storage in the CWC *L. pertusa* under an experimental pulse of (isotopically enriched) phytodetritus and a subsequent period of low food availability. For the first time, the longer term utilization of a food pulse by a CWC was followed via stable-isotope ^{13}C and ^{15}N enrichment of the food. We discuss (a) the bulk C and N cycling of the CWC after feeding and during deprivation of particulate food, (b) its tissue composition, and (c) the fate of the C and N from the phytodetritus food pulse, i.e., its release vs. storage.

Bulk carbon and nitrogen cycling

Metabolic rate

Maintained oxygen consumption (respiration) and ammonium excretion of *L. pertusa* indicate that this CWC species does not undergo a torpor, i.e., a reduction of metabolic rate, during short-term food deprivation of 4 weeks. Only a longer term food deprivation of 7 months prompts *L. pertusa* to significantly reduce its respiration rate by 39–52% (Larsson et al. 2013*a*; Baussant et al. 2017). The tolerance of *L. pertusa* to food deprivation stands in contrast to other CWC species. Naumann et al. (2011) found a strong decrease of 51% in respiration for the Mediterranean solitary CWC *Desmophyllum dianthus* after 3 weeks of food deprivation. The oxygen consumption and ammonium excretion rates of *L. pertusa* in this study are comparable to, but in the lower range of, previous laboratory and in situ studies for the same species (Table 5). *D. dianthus* shows a higher experimental respiration rate than *L. pertusa*, independent of temperature (Table 5), and may therefore respond faster to food deprivation. Nevertheless, increased temperatures, resulting from global climate change, may generally increase the respiration rates of CWCs (Dodds et al. 2007), and the resulting increased energetic demand could reinforce the effects of seasonally reduced food availability (Duineveld et al. 2004, 2007; Lavaleye et al. 2009; Guihen et al. 2018).

Organic matter release

Cold-water and warm-water corals produce mucus, a polysaccharide–protein complex, for protection against sedimentation and biofouling, and aid in food acquisition (Bythell and Wild 2011). The observed POC release rates of *L. pertusa* are comparable to the study by Wild et al. (2008). These authors, however, suggest that most of the mucoid POM quickly dissolves in seawater, resulting in a 30 times higher release of DOM than of POM (Wild et al. 2008;

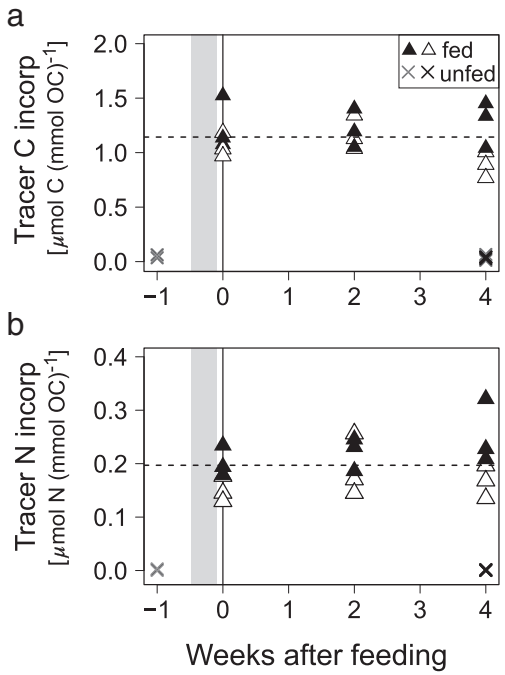

Fig. 6. Tracer carbon (**a**) and nitrogen (**b**) incorporation from the phytodetritus food pulse (gray bar) into coral tissue, per mmol OC; triangles: fed coral fragments of, respectively, two coral batches (black and white) sampled in weeks 0, 2, and 4. "x": unfed coral fragments (week 0: "Field," week 4: "Unfed controls"). Dashed line: minimum adequate model.

Naumann et al. 2014). The high DOM release rates are not observed here, and the comparatively low DOM release of *L. pertusa* challenges the (quantitative) importance of the sponge loop in CWC reefs (Rix et al. 2016). The sponge loop describes the uptake of coral-released DOM by sponges, which in turn shed detrital POM, feeding detritivores in tropical coral reefs (de Goeij et al. 2013). Rix et al. (2016) provided qualitative evidence of this loop for CWC reefs, but the large uncertainty about the amount of DOM release by *L. pertusa* warrants further research before we can infer the quantitative importance of this recycling loop in these ecosystems.

The loss of C and N as POC and PON during 4-week food deprivation amounts to 17% and 56% of their overall C and N losses, which compares favorably to a study by Larsson et al. (2013*b*). POM release thus represents a significant component of the energy budget of CWCs, which is maintained under food deprivation, underlining its important physiological role for the organism (Bythell and Wild 2011). An increase in mucus production, for instance, due to sedimentation or other stressors (Reitner 2005; Zetsche et al. 2016), is likely to have negative consequences for their energy balance, especially under temporally reduced food availability (Duineveld et al. 2004, 2007; Lavaleye et al. 2009; Guihen et al. 2018).

Tissue composition and carbon storage

Our data indicate that CWC *L. pertusa* stores carbon in neutral lipids, which represent its largest tissue carbon pool, followed by proteins and carbohydrates. NLFAs are the building blocks of triacylglycerols and wax esters, and their high contribution to the CWCs' total OC (20% to 23%) underscores the postulated C storage in this pool (Dodds et al. 2009; Larsson et al. 2013*a*). The sum of C in all measured tissue pools, however, accounts for only 40% of the total OC. Other studies on warm and CWCs find a dominance of proteins (Al-Lihaibi et al. 1998; Rossi et al. 2006; Mueller et al. 2014), which was not observed here, while lipid concentrations compare with previous studies (Dodds et al. 2009; Larsson et al. 2013*a*). Carbohydrates contribute only 1% to *L. pertusa*'s OC, which excludes them as additional important C storage pool. Invertebrates such as bivalves, which use glycogen as C-storing molecule, contain up to 50% glycogen in their tissue DM (Beukema and De Bruin 1977; Galap et al. 1997).

The 20% decrease in total OC and 13% decrease in NLFA-C during food deprivation point toward a consumption of *L. pertusa*'s tissue C stores. This trend was not statistically significant, though, due to the variability in corals' OC content, likely caused by their high background of inorganic C. The average decrease in OC and NLFA-C, however, compares favorably with the integrated 4-week C release of 10% of their total OC. A similar rate of OC decrease was observed in *L. pertusa* during a 7-month starvation period (Larsson et al. 2013*a*). The maintenance of PLFAs indicates that CWCs can preserve their membranes and tissue structure during 4 week deprivation from food.

Fate of the food pulse

Tracer release

The respiration and POM release of the food pulse peak shortly after feeding and decline slowly from week 1 to week 4. The initial peak in tracer metabolism indicates an overall increase in metabolism in response to feeding and/or a preferential metabolization of ^{13}C and ^{15}N from the food pulse. An overall increase in metabolic activity (e.g., respiration) after feeding is commonly referred to as specific dynamic action of food (reviewed by McCue 2006 and Secor 2008). A peak in (tracer) POC and PON release after feeding could indicate the release of food-derived material as fecal matter, a loss of nondigested food (Yonge 1930; Brusca and Brusca 2003), and/or an increased mucus production to retain food particles (Zetsche et al. 2016). The increase in metabolism and POM release is particularly pronounced in the tracer fluxes, suggesting that a part of the food pulse is preferentially used to "pay" for metabolic costs involved in food uptake and assimilation. The subsequently lower tracer release rate implies that the remainder of the food pulse had been incorporated in a tissue pool with a lower turnover rate.

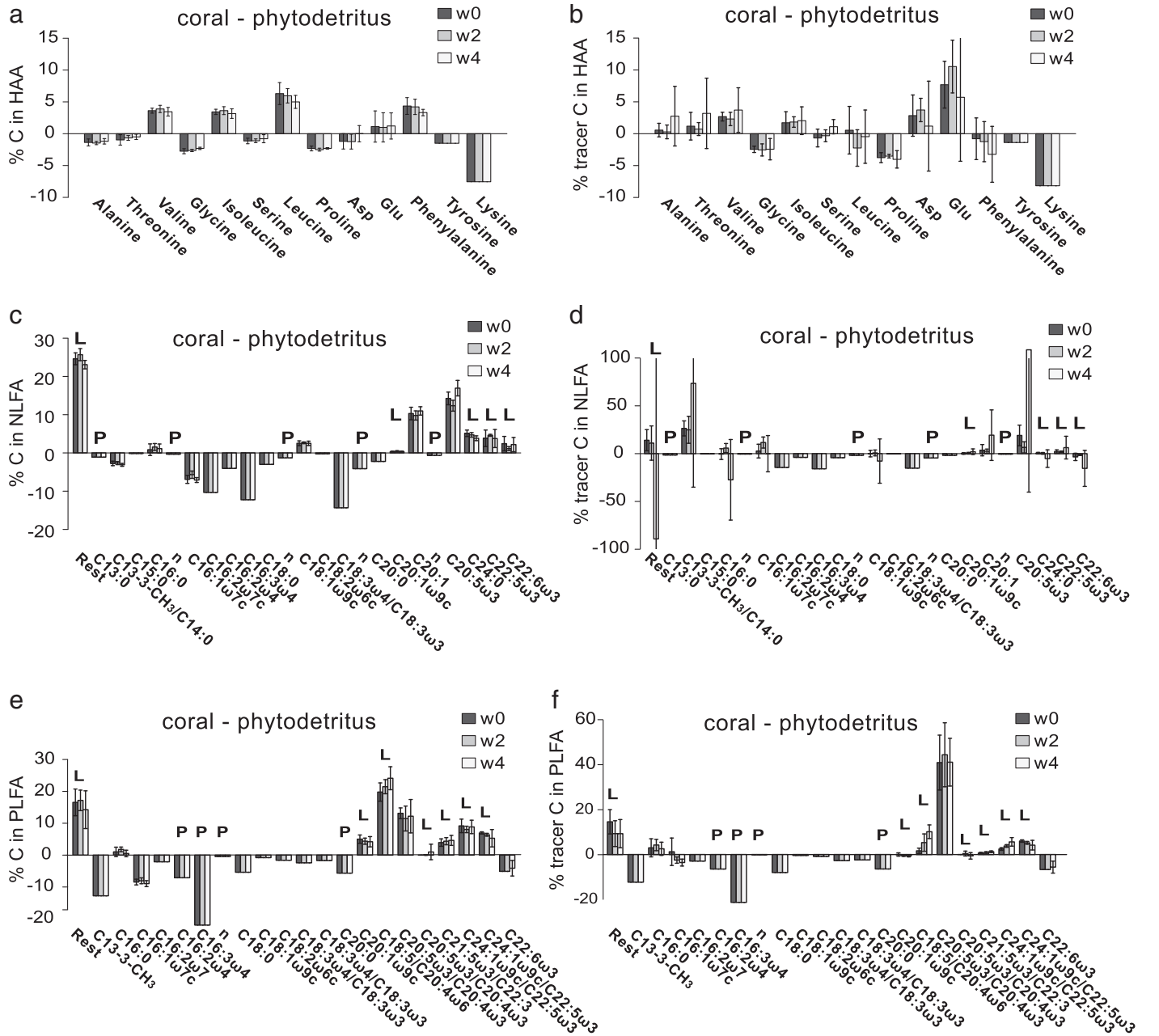

Fig. 7. Comparison of *L. pertusa* compound profiles with the phytodetritus food, shown as the difference "coral-phytodetritus." (**a**, **c**, **e**) Difference in the percentage of carbon in a compound relative to the total C in all compounds. (**b**, **d**, **f**) Difference in the percentage of (tracer) C incorporated in a compound relative to the total (tracer) C incorporated in all compounds. Positive values indicate preferential incorporation, negative values indicate preferential loss. Abbreviations: L, compound only present *in L. pertusa*; P, compound only in phytodetritus; Asp, asparagine/aspartic acid; Glu, glutamine/-glutamic acid; Rest, FAs <5% C-concentration; *n*, unknown compound.

Tracer retention

Lophelia pertusa largely retained the initially incorporated phytodetritus carbon from the food pulse throughout 4 weeks of food deprivation, which further indicates that the non-metabolized remainder of the material was integrated in a low-turnover, storage tissue pool. The daily rate of phytodetritus-C incorporation of *Lophelia pertusa* was four times higher than in previous stable isotope tracer studies (Mueller et al. 2014; Van Oevelen et al. 2016), which compares reasonably, given the differences in coral-fragment size, food concentration, and experimental setup. *L. pertusa* can maintain this incorporation rate over a wide range of resources including phytodetritus, zooplankton, bacteria, and DOM (Mueller et al. 2014) and increases food incorporation with increasing food availability (Van Oevelen et al. 2016), underlining its flexibility in resource utilization.

Table 5. Oxygen consumption and ammonium excretion rates and respective O : N indices of *L. pertusa* and *D. dianthus* measured in different studies under different temperatures.

Study	Species	Temperature (°C)	Respiration (μmol O_2 [g DM]$^{-1}$ h^{-1})	Ammonium excretion (μmol NH_4^+ [g DM]$^{-1}$ h^{-1})	O : N index
Present study	*L. pertusa*, (fed)	8	0.14±0.02	0.004±0.001	35
Khripounoff et al. (2014)	*L. pertusa,* in situ	9.6 to 10.2	0.30	0.008	41
Larsson et al. (2013*a*)	*L. pertusa*	8	Ø ca. 0.13	na	na
Larsson et al. (2013*b*)	*L. pertusa*	8	0.27±0.05	na	na
Naumann et al. (2014)	*L. pertusa*	12	1.05±0.3	0.13±0.07	10
Maier et al. (2013)	*L. pertusa*	13	0.07–0.27	na	na
Naumann et al. (2011)	*D. dianthus*	12	1.51±0.4	na	na

The rate of food incorporation in this study and Van Oevelen et al. (2016) (i.e., 0.1% to 0.5% of phytodetritus-C per 12 h) appears low compared to capture rates of (live) phytoplankton (1.3% of food items per hour; Orejas et al. 2016) and zooplankton (0.5% to 26% of food items per hour; Purser et al. 2010; Orejas et al. 2016). Incorporation rates are, however, not directly comparable with capture rates, because the latter measure does not take losses of nonassimilated food (e.g., sloppy feeding and feces production) into account. In addition, we observed aggregation and subsequent settling of the phytodetritus on the bottom of the incubation chamber, which could partly explain the relatively low food incorporation rate. Aggregation of phytodetritus is a natural phenomenon and fosters the rapid export of the larger particles to the deep sea, especially during the phytoplankton blooms (Alldredge and Gotschalk 1988; Kiørboe et al. 1990; Turner 2015). The impact of negative phytodetritus buoyancy on CWC feeding success may be counteracted by organic material resuspension due to strong bottom currents (Davies et al. 2009; Mienis et al. 2012*a*,*b*).

The tissue composition of *L. pertusa* is in imbalance with the phytodetritus composition, the latter having a considerably lower percentage of neutral lipids and higher percentage of amino acids (AAs). This imbalance is reflected in the phytodetritus incorporation, with a comparatively low incorporation of NLFAs (4% of total C incorporation) and high AA incorporation (12%). A sole phytodetritus diet may therefore not be sufficient to store up lipid reserves, and there are indications that CWCs may utilize diurnally and seasonally migrating zooplankton (Kiriakoulakis et al. 2005; Hebbeln et al. 2014; Guihen et al. 2018; Van Engeland et al. 2019), which has a high lipid content (Lee et al. 2006), in addition to phytodetrital material.

The AA composition of the phytodetritus and the corals closely match, which is evidenced by the largely unaltered incorporation of phytodetritus AAs by the coral. Preferential uptake or loss of AAs, as reported for other invertebrates (Woulds et al. 2012), was minor and only occurred for a few compounds, such as glutamic acid/glutamine and aspartic acid/asparagine. Preferential AA uptake can be related to the pathways of AA synthesis in corals, as both glutamine/glutamate and asparagine/aspartate share an important role as intermediates in the tricarboxylic acid cycle (Fitzgerald and Szmant 1997; Piniak et al. 2003). A preference of those AAs was also reported for *L. pertusa*'s AA de novo synthesis from an inorganic carbon source (Middelburg et al. 2015).

Lophelia pertusa largely used the essential short-chain MUFAs and PUFAs to build longer chain HUFAs. In this process of "trophic upgrading of FAs", marine invertebrates acquire essential "precursor" PUFAs and MUFAs such as oleic acid (C18:1ω9), linoleic acid (C18:2ω6), and linolenic acid (C18:3ω3) from marine microalgae and elongate and/or desaturate them to longer chain HUFAs such as arachidonic acid (C20:4ω6), docosapentaenoic acid and docosahexaenoic acid (C22:5ω3 and C22:6ω3), and mono-unsaturated nervonic acid (C24:1ω9c; Kelly and Scheibling 2012; Monroig et al. 2013). As most marine invertebrates, *L. pertusa* is particularly rich in eicosapentaenoic acid (EPA, C20:5ω3; Phillips 1984), which plays an important role in its membrane-forming phospholipid pool (Lee et al. 2006). The coral incorporated EPA directly (and preferentially) from the diatom-derived phytodetritus. As marine microalgae have been considered the only marine organisms capable of synthesizing essential "precursor" FAs (Dalsgaard et al. 2003), the use of those FAs as trophic markers has found a wide application in ecology (Dalsgaard et al. 2003; Iverson et al. 2004; Kelly and Scheibling 2012). A recent study, however, showed that *L. pertusa* can also synthesize linoleic acid (Mueller et al. 2014). This finding complicates the use of FA trophic markers for CWCs and indicates a partial independence of CWCs from the surface production (phytoplankton and zooplankton) for their FA metabolism.

Conclusion

This study shows for the first time that CWC *L. pertusa* is able to utilize a phytodetritus food pulse for a prolonged

period of time, by metabolizing only parts of it immediately and moving the remainder to a longer term storage pool with slower turnover. Carbon storage, most likely in neutral lipids (Dodds et al. 2009; Larsson et al. 2013*a*; this study), allows *L. pertusa* to maintain their metabolic rate during several weeks of food deprivation (Larsson et al. 2013*a*; Baussant et al. 2017; this study). Nevertheless, their FA incorporation revealed that a sole phytodetritus diet may not be sufficient to store up lipid reserves, and lipid-rich diurnally and seasonally migrating zooplankton could provide an important addition (Kiriakoulakis et al. 2005; Hebbeln et al. 2014; Guihen et al. 2018; Van Engeland et al. 2019). Besides bridging periods of reduced food supply, lipid stores are crucial to pay for seasonal reproduction, and food supply, (lipid) storage, and reproduction may undergo a close interplay which is barely understood (Brooke and Järnegren 2013). The current study underlines that *L. pertusa* is well-adapted to temporal variations in food availability. The experiment provided important knowledge of a specific simulation of the dynamic environment that CWCs thrive in, that complements in situ observations on their distribution and environmental requirements. The fine-tuned balance of resource supply and needs of deep-sea habitat-forming CWCs may be affected by global climate change, with increased temperature and stratification potentially reducing primary productivity and export production (Bopp et al. 2001; Gregg et al. 2003; Soetaert et al. 2016) and ocean acidification increasing the resource demand for increased calcification costs (Cohen and Holcomb 2009; McCulloch et al. 2012*a*,*b*; Büscher et al. 2017).

References

Alldredge, A. L., and C. Gotschalk. 1988. In situ settling behavior of marine snow. Limnol. Oceanogr. **33**: 339–351. doi:10.4319/lo.1988.33.3.0339

Al-Lihaibi, S. S., A. A. Al-Sofyani, and G. R. Niaz. 1998. Chemical composition of corals in Saudi Red Sea coast. Oceanol. Acta **21**: 495–501. doi:10.1016/S0399-1784(98)80033-9

Baussant, T., M. Nilsen, E. Ravagnan, S. Westerlund, and S. Ramanand. 2017. Physiological responses and lipid storage of the coral *Lophelia pertusa* at varying food density. J. Toxicol. Environ. Health A **80**: 1–19. doi:10.1080/15287394.2017.1297274

Beukema, J. J., and W. De Bruin. 1977. Seasonal changes in dry weight and chemical composition of the soft parts of the tellinid bivalve *Macoma balthica* in the Dutch Wadden Sea. Neth. J. Sea Res. **11**: 42–55. doi:10.1016/0077-7579(77)90020-5

Bopp, L., P. Monfray, O. Aumont, J.-L. Dufresne, H. Le Treut, G. Madec, L. Terray, and J. C. Orr. 2001. Potential impact of climate change on marine export production. Glob. Biogeochem. Cycles **15**: 81–89. doi:10.1029/1999GB001256

Boschker, H. T. S., J. F. C. de Brouwer, and T. E. Cappenberg. 1999. The contribution of macrophyte-derived organic matter to microbial biomass in salt-marsh sediments: Stable carbon isotope analysis of microbial biomarkers. Limnol. Oceanogr. **44**: 309–319. doi:10.4319/lo.1999.44.2.0309

Brooke, S., and J. Järnegren. 2013. Reproductive periodicity of the scleractinian coral *Lophelia pertusa* from the Trondheim Fjord, Norway. Mar. Biol. **160**: 139–153. doi:10.1007/s00227-012-2071-x

Brusca, R. C., and G. J. Brusca. 2003. Invertebrates, 2nd ed. Sinauer Associates.

Büscher, J., A. U. Form, and U. Riebesell. 2017. Interactive effects of ocean acidification and warming on growth, fitness and survival of the cold-water coral *Lophelia pertusa* under different food availabilities. Front. Mar. Sci. **4**: 1–14. doi:10.3389/fmars.2017.00101

Bythell, J. C., and C. Wild. 2011. Biology and ecology of coral mucus release. J. Exp. Mar. Biol. Ecol. **408**: 88–93. doi:10.1016/j.jembe.2011.07.028

Carlier, A., E. Le Guilloux, K. Olu, J. Sarrazin, F. Mastrototaro, M. Taviani, and J. Clavier. 2009. Trophic relationships in a deep Mediterranean cold-water coral bank (Santa Maria di Leuca, Ionian Sea). Mar. Ecol. Prog. Ser. **397**: 125–137. doi:10.3354/meps08361

Christiansen, B., and S. Diel-Christiansen. 1993. Respiration of lysianassoid amphipods in a subarctic fjord and some implications on their feeding ecology. Sarsia **78**: 9–15. doi:10.1080/00364827.1993.10413516

Cohen, A. L., and M. Holcomb. 2009. Why corals care about ocean acidification: Uncovering the mechanism. Oceanography **22**: 118–127. doi:10.5670/oceanog.2009.102

Crawley, M. J. 2007. The R book, 1st ed. Wiley.

Dalsgaard, J., M. S. John, G. Kattner, D. Mueller-Navarra, and W. Hagen. 2003. Fatty acid trophic markers in the pelagic marine environment, p. 225–340. *In* A. J. Southward, P. A. Tyler, C. M. Young, and L. A. Fuiman [eds.], Advances in marine biology, v. **46**. Elsevier Science Ltd.

Davies, A. J., M. Wisshak, J. C. Orr, and J. Murray Roberts. 2008. Predicting suitable habitat for the cold-water coral *Lophelia pertusa* (Scleractinia). Deep Sea Res. Part I Oceanogr. Res. Pap. **55**: 1048–1062. doi:10.1016/j.dsr.2008.04.010

Davies, A. J., G. C. A. Duineveld, M. S. S. Lavaleye, M. J. N. Bergman, H. Van Haren, and J. M. Roberts. 2009. Downwelling and deep-water bottom currents as food supply mechanisms to the cold-water coral *Lophelia pertusa* (Scleractinia) at the Mingulay reef complex. Limnol. Oceanogr. **54**: 620–629. doi:10.4319/lo.2009.54.2.0620

de Goeij, J. M., D. van Oevelen, M. J. A. Vermeij, R. Osinga, J. J. Middelburg, A. F. P. M. de Goeij, and W. Admiraal. 2013. Surviving in a marine desert: The sponge loop retains resources within coral reefs. Science **342**: 108–110. doi:10.1126/science.1241981

Dodds, L. A., J. M. Roberts, A. C. Taylor, and F. Marubini. 2007. Metabolic tolerance of the cold-water coral *Lophelia pertusa* (Scleractinia) to temperature and dissolved oxygen

change. J. Exp. Mar. Biol. Ecol. **349**: 205–214. doi:10.1016/j.jembe.2007.05.013

Dodds, L. A., K. D. Black, H. Orr, and J. M. Roberts. 2009. Lipid biomarkers reveal geographical differences in food supply to the cold-water coral *Lophelia pertusa* (Scleractinia). Mar. Ecol. Prog. Ser. **397**: 113–124. doi:10.3354/meps08143

Duineveld, G. C. A., M. S. S. Lavaleye, and E. M. Berghuis. 2004. Particle flux and food supply to a seamount cold-water coral community (Galicia Bank, NW Spain). Mar. Ecol. Prog. Ser. **277**: 13–23. doi:10.3354/meps277013

Duineveld, G. C. A., M. S. S. Lavaleye, M. J. N. Bergman, H. De Stigter, and F. Mienis. 2007. Trophic structure of a cold-water coral mound community (Rockall Bank, NE Atlantic) in relation to the near-bottom particle supply and current regime. Bull. Mar. Sci. **81**: 449–467.

Duineveld, G. C., R. M. Jeffreys, M. S. Lavaleye, A. J. Davies, M. J. Bergman, T. Watmough, and R. Witbaard. 2012. Spatial and tidal variation in food supply to shallow cold-water coral reefs of the Mingulay reef complex (outer Hebrides, Scotland). Mar. Ecol. Prog. Ser. **444**: 97–115. doi:10.3354/meps09430

Erbe, T. 1999. Die Quantifizierung von Aminosäurenisomeren in Lebensmitteln mittels chiraler Gaschromatographie-Massenspektrometrie im Hinblick auf die Relevanz und die Entstehungsmechanismen von D-Aminosäuren. Ph.D. thesis. Univ. of Giessen.

Findlay, H. S., Y. Artioli, J. Moreno Navas, S. J. Hennige, L. C. Wicks, V. A. I. Huvenne, E. M. S. Woodward, and J. M. Roberts. 2013. Tidal downwelling and implications for the carbon biogeochemistry of cold-water corals in relation to future ocean acidification and warming. Glob. Chang. Biol. **19**: 2708–2719. doi:10.1111/gcb.12256

Fitt, W. K., and R. L. Pardy. 1981. Effects of starvation, and light and dark on the energy metabolism of symbiotic and aposymbiotic sea anemones, *Anthopleura elegantissima*. Mar. Biol. **61**: 199–205. doi:10.1007/BF00386660

Fitzgerald, L. M., and A. M. Szmant. 1997. Biosynthesis of "essential" amino acids by scleractinian corals. Biochem. J. **322**: 213–221. doi:10.1042/bj3220213

Frederiksen, R., A. Jensen, and H. Westerberg. 1992. The distribution of the scleractinian coral *Lophelia pertusa* around the Faroe Islands and the relation to internal tidal mixing. Sarsia **77**: 157–171. doi:10.1080/00364827.1992.10413502

Freiwald, A. 2002. Reef-forming cold-water corals, p. 365–385. *In* G. Wefer, D. Billett, D. Hebbeln, B. B. Joergensen, M. Schlueter, and T. C. E. Van Weering [eds.], Ocean margin systems. Springer-Verlag.

Freiwald, A., J. H. Fosså, A. Grehan, T. Koslow, and J. M. Roberts. 2004. Cold-water coral reefs. UNEP-WCMC.

Gaard, E. 1999. The zooplankton community structure in relation to its biological and physical environment on the Faroe shelf, 1989-1997. J. Plankton Res. **21**: 1133–1152. doi:10.1093/plankt/21.6.1133

Galap, C., F. Leboulenger, and J.-P. Grillot. 1997. Seasonal variation in biochemical constituents during the reproductive cycle of the female dog cockle *Glycymeris glycymeris*. Mar. Biol. **129**: 625–634. doi:10.1007/s002270050205

Glud, R. N., B. D. Eyre, and N. Patten. 2008. Biogeochemical responses to mass coral spawning at the great barrier reef: Effects on respiration and primary production. Limnol. Oceanogr. **53**: 1014–1024. doi:10.4319/lo.2008.53.3.1014

González-Gil, R., F. G. Taboada, J. Höfer, and R. Anadón. 2015. Winter mixing and coastal upwelling drive long-term changes in zooplankton in the Bay of Biscay (1993–2010). J. Plankton Res. **37**: 337–351. doi:10.1093/plankt/fbv001

Gregg, W. W., M. E. Conkright, P. Ginoux, J. E. O'Reilly, and N. W. Casey. 2003. Ocean primary production and climate: Global decadal changes. Geophys. Res. Lett. **30**: 1809. doi:10.1029/2003GL016889

Grosse, J., P. van Breugel, and H. T. S. Boschker. 2015. Tracing carbon fixation in phytoplankton-compound specific and total ^{13}C incorporation rates. Limnol. Oceanogr. Methods **13**: 288–302. doi:10.1002/lom3.10025

Guihen, D., M. White, and T. Lundälv. 2018. Zooplankton drive diurnal changes in oxygen concentration at Tisler cold-water coral reef. Coral Reefs **37**: 1013–1025. doi:**10**.1007/s00338-018-1711-0

Heath, M. R., and S. H. Jónasdóttir. 2003. Distribution and abundance of overwintering *Calanus finmarchicus* in the Faroe–Shetland Channel. Fish. Oceanogr. **8**: 40–60. doi:10.1046/j.1365-2419.1999.00012.x

Hebbeln, D., and others. 2014. Environmental forcing of the Campeche cold-water coral province, southern Gulf of Mexico. Biogeosciences **11**: 1799–1815. doi:10.5194/bg-11-1799-2014

Iverson, S. J., C. Field, W. Don Bowen, and W. Blanchard. 2004. Quantitative fatty acid signature analysis: A new method of estimating predator diets. Ecol. Monogr. **74**: 211–235. doi:10.1890/02-4105

Jónasdóttir, S. H., A. W. Visser, K. Richardson, and M. R. Heath. 2015. Seasonal copepod lipid pump promotes carbon sequestration in the deep North Atlantic. Proc. Natl. Acad. Sci. USA **112**: 12122–12126. doi:10.1073/pnas.1512110112

Jonsson, L. G., P. G. Nilsson, F. Floruta, and T. Lundälv. 2004. Distributional patterns of macro- and megafauna associated with a reef of the cold-water coral *Lophelia pertusa* on the Swedish west coast. Mar. Ecol. Prog. Ser. **284**: 163–171. doi:10.3354/meps284163

Karl, D. M., G. A. Knauer, and J. H. Martin. 1988. Downward flux of particulate organic matter in the ocean: A particle decomposition paradox. Nature **332**: 438–441. doi:10.1038/332438a0

Kelly, J. R., and R. E. Scheibling. 2012. Fatty acids as dietary tracers in benthic food webs. Mar. Ecol. Prog. Ser. **446**: 1–22. doi:10.3354/meps09559

Khripounoff, A., J.-C. Caprais, J. Le Bruchec, P. Rodier, P. Noel, and C. Cathalot. 2014. Deep cold-water coral ecosystems in the Brittany submarine canyons (Northeast Atlantic): Hydrodynamics, particle supply, respiration, and carbon

cycling. Limnol. Oceanogr. **59**: 87–98. doi: 10.4319/lo.2014.59.01.0087

Kiørboe, T., K. P. Andersen, and H. G. Dam. 1990. Coagulation efficiency and aggregate formation in marine phytoplankton. Mar. Biol. **107**: 235–245. doi:10.1007/BF01319822

Kiriakoulakis, K., E. Fisher, G. Wolff, A. Freiwald, A. Grehan, and J. Roberts. 2005. Lipids and nitrogen isotopes of two deep-water corals from the north-East Atlantic: Initial results and implications for their nutrition, p. 715–729. *In* A. Freiwald and J. Roberts [eds.], Cold-water corals and ecosystems. Springer.

Kopp, C., I. Domart-Coulon, S. Escrig, B. M. Humbel, M. Hignette, and A. Meibom. 2015. Subcellular investigation of photosynthesis-driven carbon and nitrogen assimilation and utilization in the symbiotic reef coral *Pocillopora damicornis*. MBio **6**: 1–9. doi:10.1128/mBio.02299-14

Larsson, A. I., T. Lundälv, and D. van Oevelen. 2013*a*. Skeletal growth, respiration rate and fatty acid composition in the cold-water coral *Lophelia pertusa* under varying food conditions. Mar. Ecol. Prog. Ser. **483**: 169–184. doi:10.3354/meps10284

Larsson, A. I., D. van Oevelen, A. Purser, and L. Thomsen. 2013*b*. Tolerance to long-term exposure of suspended benthic sediments and drill cuttings in the cold-water coral *Lophelia pertusa*. Mar. Pollut. Bull. **70**: 176–188. doi:10.1016/j.marpolbul.2013.02.033

Lavaleye, M., G. Duineveld, T. Lundälv, M. White, D. Guihen, K. Kiriakoulakis, and G. A. Wolff. 2009. Cold-water corals on the Tisler reef. Oceanography **22**: 76–84. doi:10.5670/oceanog.2009.08

Lee, R. F., W. Hagen, and G. Kattner. 2006. Lipid storage in marine zooplankton. Mar. Ecol. Prog. Ser. **307**: 273–306. doi:10.3354/meps307273

Linke, P. 1992. Metabolic adaptation of deep-sea benthic foraminifera to seasonally varying food input. Mar. Ecol. Prog. Ser. **81**: 51–63. doi:10.3354/meps081051

Maier, C., F. Bils, M. G. Weinbauer, P. Watremez, M. A. Peck, and J.-P. Gattuso. 2013. Respiration of Mediterranean cold-water corals is not affected by ocean acidification as projected for the end of the century. Biogeosciences **10**: 5671–5680. doi: 10.5194/bg-10-5671-2013

McCue, M. D. 2006. Specific dynamic action: A century of investigation. Comp. Biochem. Physiol. A Mol. Integr. Physiol. **144**: 381–394. doi:10.1016/j.cbpa.2006.03.011

McCulloch, M., J. Falter, J. Trotter, and P. Montagna. 2012*a*. Coral resilience to ocean acidification and global warming through pH up-regulation. Nat. Clim. Chang. **2**: 623–627. doi:10.1038/nclimate1473

McCulloch, M., and others. 2012*b*. Resilience of cold-water scleractinian corals to ocean acidification: Boron isotopic systematics of pH and saturation state up-regulation. Geochim. Cosmochim. Acta **87**: 21–34. doi:10.1016/j.gca.2012.03.027

Middelburg, J. J., C. E. Mueller, B. Veuger, A. I. Larsson, A. Form, and D. van Oevelen. 2015. Discovery of symbiotic nitrogen fixation and chemoautotrophy in cold-water corals. Sci. Rep. **5**: 1–9. doi:10.1038/srep17962

Mienis, F., H. C. de Stigter, M. White, G. Duineveld, H. de Haas, and T. C. E. van Weering. 2007. Hydrodynamic controls on cold-water coral growth and carbonate-mound development at the SW and SE Rockall trough margin, NE Atlantic Ocean. Deep-Sea Res. I Oceanogr. Res. Pap. **54**: 1655–1674. doi:10.1016/j.dsr.2007.05.013

Mienis, F., G. C. A. Duineveld, A. J. Davies, S. W. Ross, H. Seim, J. Bane, and T. C. E. Van Weering. 2012*a*. The influence of near-bed hydrodynamic conditions on cold-water corals in the Viosca knoll area, Gulf of Mexico. Deep-Sea Res. Part I Oceanogr. Res. Pap. **60**: 32–45. doi:10.1016/j.dsr.2011.10.007

Mienis, F., H. C. De Stigter, H. De Haas, C. Van der Land, and T. C. E. Van Weering. 2012*b*. Hydrodynamic conditions in a cold-water coral mound area on the Renard ridge southern Gulf of Cadiz. J. Mar. Syst. **96**: 61–71. doi:10.1016/j.jmarsys.2012.02.002

Monroig, O., D. R. Tocher, and J. C. Navarro. 2013. Biosynthesis of polyunsaturated fatty acids in marine invertebrates: Recent advances in molecular mechanisms. Mar. Drugs **11**: 3998–4018. doi:10.3390/md11103998

Moodley, L., H. T. S. Boschker, J. J. Middelburg, R. Pel, P. M. J. Herman, E. M. G. T. De Deckere, and C. H. R. Heip. 2000. Ecological significance of benthic foraminifera: ^{13}C labelling experiments. Mar. Ecol. Prog. Ser. **202**: 289–295. doi:10.3354/meps202289

Mortensen, P. B., T. Hovland, J. H. Fosså, and D. M. Furevik. 2001. Distribution, abundance and size of *Lophelia pertusa* coral reefs in mid-Norway in relation to seabed characteristics. J. Mar. Biol. Assoc. UK **81**: 581–597. doi:10.1017/S002531540100426X

Mueller, C. E., A. I. Larsson, B. Veuger, J. J. Middelburg, and D. Van Oevelen. 2014. Opportunistic feeding on various organic food sources by the cold-water coral *Lophelia pertusa*. Biogeosciences **11**: 123–133. doi:10.5194/bg-11-123-2014

Naumann, M. S., C. Orejas, C. Wild, and C. Ferrier-Pages. 2011. First evidence for zooplankton feeding sustaining key physiological processes in a scleractinian cold-water coral. J. Exp. Biol. **214**: 3570–3576. doi:10.1242/jeb.061390

Naumann, M. S., C. Orejas, and C. Ferrier-Pagès. 2014. Species-specific physiological response by the cold-water corals *Lophelia pertusa* and *Madrepora oculata* to variations within their natural temperature range. Deep-Sea Res. Part II Top. Stud. Oceanogr. **99**: 36–41. doi:10.1016/j.dsr2.2013.05.025

Orejas, C., and others. 2016. The effect of flow speed and food size on the capture efficiency and feeding behaviour of the cold-water coral *Lophelia pertusa*. J. Exp. Mar. Biol. Ecol. **481**: 34–40. doi:10.1016/j.jembe.2016.04.002

Ortega, M. M., J. M. Lopez de Pariza, and E. Navarro. 1988. Seasonal changes in the biochemical composition and oxygen consumption of the sea anemone *Actinia equina* as

related to body size and shore level. Mar. Biol. **97**: 137–143. doi:10.1007/BF00391253

Phillips, N. W. 1984. Role of different microbes and substrates as potential suppliers of specific, essential nutrients to marine detritivores. Bull. Mar. Sci. **35**: 283–298.

Pinheiro, J., D. Bates, S. DebRoy, D. Sarkar, and R Core Team. 2017. NLME: Linear and nonlinear mixed effects models. R package version 3.1–131.

Piniak, G. A., F. Lipschultz, and J. McClelland. 2003. Assimilation and partitioning of prey nitrogen within two anthozoans and their endosymbiotic zooxanthellae. Mar. Ecol. Prog. Ser. **262**: 125–136. doi:10.3354/meps262125

Purser, A., A. I. Larsson, L. Thomsen, and D. van Oevelen. 2010. The influence of flow velocity and food concentration on *Lophelia pertusa* (Scleractinia) zooplankton capture rates. J. Exp. Mar. Biol. Ecol. **395**: 55–62. doi:10.1016/j.jembe.2010.08.013

R Core Team 2017. R: A language and environment for statistical computing. R Foundation for Statistical Computing, Vienna, Austria. URL https://www.R-project.org/.

Reitner, J. 2005. Calcifying extracellular mucus substances (EMS) of *Madrepora oculata*—a first geobiological approach, p. 731–744. *In* A. Freiwald and J. M. Roberts [eds.], Cold-water corals and ecosystems. Springer.

Rix, L., and others. 2016. Coral mucus fuels the sponge loop in warm- and cold-water coral reef ecosystems. Sci. Rep. **6**: 1–11. doi:10.1038/srep18715

Roberts, J. M., A. J. Wheeler, and A. Freiwald. 2006. Reefs of the deep: The biology and geology of cold-water coral ecosystems. Science **312**: 543–547. doi:10.1126/science.1119861

Rossi, S., J.-M. Gili, R. Coma, C. Linares, A. Gori, and N. Vert. 2006. Temporal variation in protein, carbohydrate, and lipid concentrations in *Paramuricea clavata* (Anthozoa, Octocorallia): Evidence for summer–autumn feeding constraints. Mar. Biol. **149**: 643–651. doi:10.1007/s00227-005-0229-5

Searle, P. L. 1984. The Berthelot or indophenol reaction and its use in the analytical chemistry of nitrogen. A review. Analyst **109**: 549–568. doi:10.1039/AN9840900549

Secor, S. M. 2008. Specific dynamic action: A review of the postprandial metabolic response. J. Comp. Physiol. B. **179**: 1–56. doi:10.1007/s00360-008-0283-7

Sieburth, J. M., V. Smetacek, and J. Lenz. 1978. Pelagic ecosystem structure: Heterotrophic components of the plankton and their relationship to plankton size-fractions. Limnol. Oceanogr. **23**: 1256–1263. doi:10.4319/lo.1978.23.6.1256

Smith, K. L., and R. J. Baldwin. 1982. Scavenging deep-sea amphipods: Effects of food odor on oxygen consumption and a proposed metabolic strategy. Mar. Biol. **68**: 287–298. doi:10.1007/BF00409595

Soetaert, K., C. Mohn, A. Rengstorf, A. Grehan, and D. van Oevelen. 2016. Ecosystem engineering creates a direct nutritional link between 600-m deep cold-water coral mounds and surface productivity. Sci. Rep. **6**: 35057. doi:10.1038/srep35057

Suess, E. 1980. Particulate organic carbon flux in the oceans—surface productivity and oxygen utilization. Nature **288**: 260–263. doi:10.1038/288260a0

Thiem, Ø., E. Ravagnan, J. H. Fosså, and J. Berntsen. 2006. Food supply mechanisms for cold-water corals along a continental shelf edge. J. Mar. Syst. **60**: 207–219. doi:10.1016/j.jmarsys.2005.12.004

Turner, J. T. 2015. Zooplankton fecal pellets, marine snow, phytodetritus and the ocean's biological pump. Prog. Oceanogr. **130**: 205–248. doi:10.1016/j.pocean.2014.08.005

Uhle, M. E., S. A. Macko, H. J. Spero, M. H. Engel, and D. W. Lea. 1997. Sources of carbon and nitrogen in modern planktonic foraminifera: The role of algal symbionts as determined by bulk and compound specific stable isotopic analyses. Org. Geochem. **27**: 103–113. doi:10.1016/S0146-6380(97)00075-2

Van Engeland, T., O. R. Godø, E. Johnsen, G. C. A. Duineveld, and D. van Oevelen. 2019. Cabled ocean observatory data reveal food supply mechanisms to a cold-water coral reef. Prog. Oceanogr. **172**: 51–64. doi: 10.1016/j.pocean.2019.01.007

Van Oevelen, D., G. Duineveld, M. Lavaleye, F. Mienis, K. Soetaert, and C. H. R. Heip. 2009. The cold-water coral community as hotspot of carbon cycling on continental margins: A food-web analysis from Rockall Bank (Northeast Atlantic). Limnol. Oceanogr. **54**: 1829–1844. doi:10.4319/lo.2009.54.6.1829

Van Oevelen, D., C. E. Mueller, T. Lundaelv, and J. J. Middelburg. 2016. Food selectivity and processing by the cold-water coral *Lophelia pertusa*. Biogeosciences **13**: 5789–5798. doi:10.5194/bg-13-5789-2016

Veuger, B., J. J. Middelburg, H. T. S. Boschker, and M. Houtekamer. 2005. Analysis of ^{15}N incorporation into D-alanine: A new method for tracing nitrogen uptake by bacteria. Limnol. Oceanogr. Methods **3**: 230–240. doi:10.4319/lom.2005.3.230

White, M., G. A. Wolff, T. Lundälv, D. Guihen, K. Kiriakoulakis, M. Lavaleye, and G. Duineveld. 2012. Cold-water coral ecosystem (Tisler reef, Norwegian shelf) may be a hotspot for carbon cycling. Mar. Ecol. Prog. Ser. **465**: 11–23. doi:10.3354/meps09888

Wiborg, K. F. 1954. Investigations on zooplankton in coastal and offshore waters of Western and Northwestern Norway—with special reference to the copepods. Report on Norwegian Fishery and Marine Investigation. Director of Fisheries. A. S John Griegs Boktrykkeri, Bergen.

Wild, C., C. Mayr, L. Wehrmann, S. Schöttner, M. Naumann, F. Hoffmann, and H. T. Rapp. 2008. Organic matter release by cold water corals and its implication for fauna-microbe interaction. Mar.Ecol.Prog.Ser.**372**:67–75.doi:10.3354/meps07724

Woulds, C., J. J. Middelburg, and G. L. Cowie. 2012. Alteration of organic matter during infaunal polychaete gut passage and links to sediment organic geochemistry. Part I: Amino acids. Geochim. Cosmochim. Acta **77**: 396–414. doi:10.1016/j.gca.2011.10.042

Yonge, C. M. 1930. Studies on the physiology of corals: 1. Feeding mechanisms and food. Gt. Barrier reef Exped. 1928-29. Sci. Rep. **1**: 1–57.

Zamer, W. E., and R. J. Hoffmann. 1993. Pyruvate metabolism in laboratory-acclimated and freshly collected sea anemones, *Metridium senile* L. J. Exp. Mar. Biol. Ecol. **171**: 23–37. doi:10.1016/0022-0981(93)90137-D

Zetsche, E. M., T. Baussant, F. J. R. Meysman, and D. Van Oevelen. 2016. Direct visualization of mucus production by the cold-water coral *Lophelia pertusa* with digital holographic microscopy. PLoS One **11**: e0146766. doi:10.1371/journal.pone.0146766

Acknowledgments

We are grateful to the staff of the IMR field station on the island of Austevoll, especially to Cathinka Krogness, for fieldwork assistance and logistical support. Funding was provided by the Netherlands Organisation for Scientific Research (VIDI grant 864.13.007 to D.v.O.) and the Norwegian Research Council (RCN project 244604/E40 to T.K.). Laurine Burdorf has provided the R package for the analysis of oxygen consumption. The analytical lab of NIOZ, especially Jan Peene, has carried out nutrient analyses, and Tanja Stratmann has assisted with the set-up of diatom cultures. Thanks to the two reviewers who provided constructive feedback on the manuscript.

Conflict of Interest

None declared.

Submitted 19 September 2018
Revised 07 December 2018
Accepted 22 January 2019

Associate editor: Ronnie Glud